

**Mitochondrial respiratory states and rates:  
Building blocks of mitochondrial physiology  
Part 1.**

[http://www.mitoeagle.org/index.php/MitoEAGLE\\_preprint\\_2018-02-08](http://www.mitoeagle.org/index.php/MitoEAGLE_preprint_2018-02-08)

Preprint version 24 (2018-02-13)

**MitoEAGLE Network**

Corresponding author: Gnaiger E

Contributing co-authors

Ahn B, Alves MG, Amati F, Aral C, Arandarčikaitė O, Åsander Frostner E, Bailey DM, Bastos Sant'Anna Silva AC, Battino M, Beard DA, Ben-Shachar D, Bishop D, Breton S, Brown GC, Brown RA, Buettner GR, Calabria E, Cardoso LHD, Carvalho E, Casado Pinna M, Cervinkova Z, Chang SC, Chicco AJ, Chinopoulos C, Coen PM, Collins JL, Crisóstomo L, Davis MS, Dias T, Distefano G, Doerrier C, Drahotka Z, Duchon MR, Ehinger J, Elmer E, Endlicher R, Fell DA, Ferko M, Ferreira JCB, Filipovska A, Fisar Z, Fisher J, Garcia-Roves PM, Garcia-Souza LF, Genova ML, Gonzalo H, Goodpaster BH, Gorr TA, Grefte S, Han J, Harrison DK, Hellgren KT, Hernansanz P, Holland O, Hoppel CL, Houstek J, Hunger M, Iglesias-Gonzalez J, Irving BA, Iyer S, Jackson CB, Jadiya P, Jansen-Dürr P, Jespersen NR, Jha RK, Kaambre T, Kane DA, Kappler L, Karabatsiakos A, Keijer J, Keppner G, Komlodi T, Kopitar-Jerala N, Krako Jakovljevic N, Kuang J, Kucera O, Labieniec-Watala M, Lai N, Laner V, Larsen TS, Lee HK, Lemieux H, Lerfall J, Lucchinetti E, MacMillan-Crow LA, Makrečka-Kuka M, Meszaros AT, Michalak S, Moiso N, Molina AJA, Montaigne D, Moore AL, Moreira BP, Mracek T, Muntane J, Muntean DM, Murray AJ, Nedergaard J, Nemeč M, Newsom S, Nozickova K, O'Gorman D, Oliveira PF, Oliveira PJ, Orynbayeva Z, Pak YK, Palmeira CM, Patel HH, Pecina P, Pereira da Silva Grilo da Silva F, Pesta D, Petit PX, Pichaud N, Pirkmajer S, Porter RK, Pranger F, Prochownik EV, Puurand M, Radenkovic F, Reboredo P, Renner-Sattler K, Robinson MM, Rohlena J, Røslund GV, Rossiter HB, Rybacka-Mossakowska J, Saada A, Salvadego D, Scatena R, Schartner M, Scheibye-Knudsen M, Schilling JM, Schlattner U, Schoenfeld P, Scott GR, Shabalina IG, Sharma P, Shevchuk I, Siewiera K, Singer D, Sobotka O, Spinazzi M, Stankova P, Stier A, Stocker R, Sumbalova Z, Suravajhala P, Tanaka M, Tandler B, Tepp K, Tomar D, Towheed A, Tretter L, Trivigno C, Tronstad KJ, Trougakos IP, Tyrrell DJ, Urban T, Velika B, Vendelin M, Vercesi AE, Victor VM, Villena JA, Wagner BA, Ward ML, Watala C, Wei YH, Wieckowski MR, Wohlwend M, Wolff J, Wuest RCI, Zaugg K, Zaugg M, Zorzano A

Supporting co-authors:

Bakker BM, Bernardi P, Boetker HE, Borsheim E, Borutaitė V, Bouitbir J, Calbet JA, Calzia E, Chaurasia B, Clementi E, Coker RH, Collin A, Das AM, De Palma C, Dubouchaud H, Durham WJ, Dyrstad SE, Engin AB, Fornaro M, Gan Z, Garlid KD, Garten A, Gourlay CW, Granata C, Haas CB, Haavik J, Haendeler J, Hand SC, Hepple RT, Hickey AJ, Hoel F, Jang DH, Kainulainen H, Khamoui AV, Klingenspor M, Koopman WJH, Kowaltowski AJ, Krajcova A, Lane N, Lenaz G, Malik A, Markova M, Mazat JP, Menze MA, Methner A, Neuzil J, Oliveira MT, Pallotta ML, Parajuli N, Pettersen IKN, Porter C, Pulnilkunnil T, Ropelle ER, Salin K, Sandi C, Sazanov LA, Silber AM, Skolik R, Smenes BT, Soares FAA, Sokolova I, Sonkar VK, Swerdlow RH, Szabo I, Trifunovic A, Thyfault JP, Valentine JM, Vieyra A, Votion DM, Williams C, Zischka H

**Updates and discussion:**

[http://www.mitoeagle.org/index.php/MitoEAGLE\\_preprint\\_2018-02-08](http://www.mitoeagle.org/index.php/MitoEAGLE_preprint_2018-02-08)

Correspondence: Gnaiger E

Department of Visceral, Transplant and Thoracic Surgery, D. Swarovski Research Laboratory, Medical University of Innsbruck, Innrain 66/4, A-6020 Innsbruck, Austria

Email: erich.gnaiger@i-med.ac.at

Tel: +43 512 566796, Fax: +43 512 566796 20

This manuscript on 'Mitochondrial respiratory states and rates' is a position statement in the frame of COST Action CA15203 MitoEAGLE. The list of co-authors evolved beyond **phase 1** (phase 1 versions 1 – 44) in the **bottom-up** spirit of COST.

This is an open invitation to scientists and students to join as co-authors, to provide a balanced view on mitochondrial respiratory control and a consensus statement on reporting data of mitochondrial respiration in terms of metabolic flows and fluxes.

**Phase 2: MitoEAGLE preprint 'The protonmotive force and respiratory control' (Versions 01 – 21):** We continue to invite comments and suggestions, particularly if you are an **early career investigator adding an open future-oriented perspective**, or an **established scientist providing a balanced historical basis**. Your critical input into the quality of the manuscript will be most welcome, improving our aims to be educational, general, consensus-oriented, and practically helpful for students working in mitochondrial respiratory physiology. **2017-11-11: Print version for MiP2017 and MitoEAGLE workshop in Hradec Kralove:**

» [http://www.mitoeagle.org/index.php/MiP2017\\_Hradec\\_Kralove\\_CZ](http://www.mitoeagle.org/index.php/MiP2017_Hradec_Kralove_CZ)

**Phase 3 (Versions 22 –): Discussion of manuscript submission to a preprint server—such as BioRxiv; invite further opinion leaders:** To join as a co-author, please feel free to focus on a particular section, providing direct input and references, and contributing to the scope of the manuscript from the perspective of your expertise. Your comments will be largely posted on the discussion page of the MitoEAGLE preprint website.

If you prefer to submit comments in the format of a referee's evaluation rather than a contribution as a co-author, I will be glad to distribute your views to the updated list of co-authors for a balanced response. We would ask for your consent on this open bottom-up policy.

**Phase 4: Journal submission.** We plan a series of follow-up reports by the expanding MitoEAGLE Network, to increase the scope of recommendations on harmonization and facilitate global communication and collaboration. Further discussions: MitoEAGLE Working Group Meetings, various conferences (EBEC 2018 in Budapest).

» [http://www.mitoglobal.org/index.php/EBEC2018\\_Budapest\\_HU](http://www.mitoglobal.org/index.php/EBEC2018_Budapest_HU)

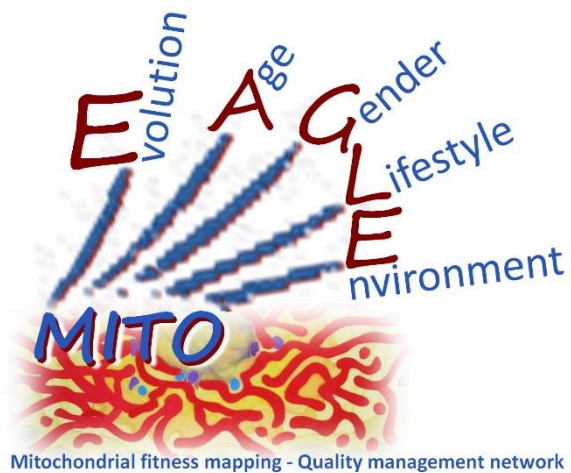
I thank you in advance for your feedback.

With best wishes,

Erich Gnaiger

Chair Mitochondrial Physiology Society – <http://www.mitophysiology.org>

Chair COST Action MitoEAGLE – <http://www.mitoeagle.org>



Mitochondrial fitness mapping - Quality management network

52  
53  
54  
55  
56  
57  
58  
59  
60  
61  
62  
63  
64  
65  
66  
67  
68  
69  
70  
71  
72  
73  
74  
75  
76  
77  
78  
79  
80  
81  
82  
83  
84  
85  
86  
87  
88  
89  
90  
91  
92  
93  
94  
95  
96  
97  
98  
99  
100

101	<b>Contents</b>
102	<b>1. Introduction</b> – Box 1: In brief: Mitochondria and Bioblasts
103	<b>2. Oxidative phosphorylation and coupling states in mitochondrial preparations</b>
104	Mitochondrial preparations
105	2.1. <i>Three coupling states of mitochondrial preparations and residual oxygen consumption</i>
106	Respiratory capacities in coupling control states
107	Kinetic control
108	The steady-state
109	Specification of biochemical dose
110	Phosphorylation, P»
111	Coupling
112	Uncoupling
113	LEAK, OXPHOS, ET, ROX
114	2.2. <i>Coupling states and respiratory rates</i>
115	P»/O <sub>2</sub> ratio
116	Control and regulation
117	Respiratory control and response
118	Respiratory coupling control
119	ET-pathway control states
120	2.3. <i>Classical terminology for isolated mitochondria</i>
121	States 1–5
122	<b>3. Normalization: fluxes and flows</b>
123	3.1. <i>Normalization: system or sample</i>
124	Flow per system, $I$
125	Extensive quantities
126	Size-specific quantities
127	– Box 2: Metabolic fluxes and flows: vectorial and scalar
128	3.2. <i>Normalization for system-size: flux per chamber volume</i>
129	System-specific flux, $J$
130	3.3. <i>Normalization: per sample</i>
131	Sample concentration, $C_{mX}$
132	Mass-specific flux, $J_{mX,O_2}$
133	Number concentration, $C_{NX}$
134	Flow per object, $I_{X,O_2}$
135	3.4. <i>Normalization for mitochondrial content</i>
136	Mitochondrial concentration, $C_{mtE}$ , and mitochondrial markers
137	Mitochondria-specific flux, $J_{mtE,O_2}$
138	3.5. <i>Evaluation of mitochondrial markers</i>
139	3.6. <i>Conversion: units</i>
140	<b>4. Conclusions</b>
141	<b>5. References</b> – Box 3: Mitochondrial and cell respiration
142	

143 **Abstract** As the knowledge base and importance of mitochondrial physiology to human health  
144 expand, the necessity for harmonizing nomenclature concerning mitochondrial respiratory  
145 states and rates has become increasingly apparent. Clarity of concept and consistency of  
146 nomenclature are key trademarks of a research field. These trademarks facilitate effective  
147 transdisciplinary communication, education, and ultimately further discovery. Peter Mitchell's  
148 chemiosmotic theory establishes the link between vectorial and scalar energy transformation  
149 and coupling in oxidative phosphorylation. The unifying concept of the protonmotive force  
150 provides the framework for developing a consistent theory and nomenclature for mitochondrial  
151 physiology and bioenergetics. Herein, we follow IUPAC guidelines on general terms of  
152 physical chemistry, extended by considerations on open systems and irreversible  
153 thermodynamics. We align the nomenclature and symbols of classical bioenergetics with a  
154 concept-driven constructive terminology to express the meaning of each quantity clearly and  
155 consistently. In this position statement, in the frame of COST Action MitoEAGLE, we  
156 endeavour to provide a balanced view on mitochondrial respiratory control and a critical  
157 discussion on reporting data of mitochondrial respiration in terms of metabolic flows and fluxes.  
158 Uniform standards for evaluation of respiratory states and rates will ultimately support the  
159 development of databases of mitochondrial respiratory function in species, tissues, and cells.

160

161 *Keywords:* Mitochondrial respiratory control, coupling control, mitochondrial  
162 preparations, protonmotive force, oxidative phosphorylation, OXPHOS, efficiency, electron  
163 transfer, ET; proton leak, LEAK, residual oxygen consumption, ROX, State 2, State 3, State 4,  
164 normalization, flow, flux

165

166

---

## 167 **Executive summary**

168

169 *See:*

170

171 [http://www.mitoeagle.org/index.php/MitoEAGLE\\_preprint\\_2018-02-08#Executive\\_summary](http://www.mitoeagle.org/index.php/MitoEAGLE_preprint_2018-02-08#Executive_summary)

172

173

---

174

175

176

177  
178  
179  
180  
181  
182  
183  
184  
185  
186  
187  
188  
189  
190  
191  
192  
193  
194  
195  
196  
197  
198  
199  
200  
201  
202  
203  
204  
205  
206  
207  
208  
209  
210  
211  
212  
213  
214  
215  
216  
217  
218  
219  
220  
221  
222  
223  
224  
225  
226  
227

---

**Box 1: In brief – Mitochondria and Bioblasts**

**Mitochondria** are the oxygen-consuming electrochemical generators evolved from endosymbiotic bacteria (Margulis 1970; Lane 2005). They were described by Richard Altmann (1894) as ‘bioblasts’, which include not only the mitochondria as presently defined, but also symbiotic and free-living bacteria. The word ‘mitochondria’ (Greek mitos: thread; chondros: granule) was introduced by Carl Benda (1898).

Mitochondrial dysfunction is associated with a wide variety of genetic and degenerative diseases. Robust mitochondrial function is supported by physical exercise and caloric balance, and is central for sustained metabolic health throughout life. Therefore, a more consistent presentation of mitochondrial physiology will improve our understanding of the etiology of disease, the diagnostic repertoire of mitochondrial medicine, with a focus on protective medicine, lifestyle and healthy aging.

We now recognize mitochondria as dynamic organelles with a double membrane that are contained within eukaryotic cells. The mitochondrial inner membrane (mtIM) shows dynamic tubular to disk-shaped cristae that separate the mitochondrial matrix, *i.e.*, the negatively charged internal mitochondrial compartment, and the intermembrane space; the latter being positively charged and enclosed by the mitochondrial outer membrane (mtOM). The mtIM contains the non-bilayer phospholipid cardiolipin, which is not present in any other eukaryotic cellular membrane. Cardiolipin promotes the formation of respiratory supercomplexes, which are supramolecular assemblies based upon specific, though dynamic, interactions between individual respiratory complexes (Greggio *et al.* 2017; Lenaz *et al.* 2017). Membrane fluidity exerts an influence on functional properties of proteins incorporated in the membranes (Waczulikova *et al.* 2007).

Mitochondria are the structural and functional elements of cell respiration. Cell respiration is the consumption of oxygen by electron transfer coupled to electrochemical proton translocation across the mtIM. In the process of oxidative phosphorylation (OXPHOS), the reduction of O<sub>2</sub> is electrochemically coupled to the transformation of energy in the form of adenosine triphosphate (ATP; Mitchell 1961, 2011). Mitochondria are the powerhouses of the cell which contain the machinery of the OXPHOS-pathways, including transmembrane respiratory complexes—proton pumps with FMN, Fe-S and cytochrome *b*, *c*, *aa*<sub>3</sub> redox systems); alternative dehydrogenases and oxidases; the coenzyme ubiquinone (Q); F<sub>1</sub>F<sub>0</sub>-ATPase or ATP synthase; the enzymes of the tricarboxylic acid cycle and the fatty acid oxidation enzymes; transporters of ions, metabolites and co-factors; and mitochondrial kinases related to energy transfer pathways. The mitochondrial proteome comprises over 1,200 proteins (Calvo *et al.* 2015; 2017), mostly encoded by nuclear DNA (nDNA), with a variety of functions, many of which are relatively well known (*e.g.*, apoptosis-regulating proteins), while others are still under investigation, or need to be identified (*e.g.*, alanine transporter).

There is a constant crosstalk between mitochondria and the other cellular components. The crosstalk between mitochondria and endoplasmic reticulum is involved in the regulation of calcium homeostasis, cell division, autophagy, differentiation, anti-viral signaling (Murley and Nunnari 2016). Cellular mitostasis is maintained through regulation at both the transcriptional and post-translational level, and through cell signalling including proteostatic (*e.g.*, the ubiquitin-proteasome and autophagy-lysosome pathways) and genome stability modules throughout the cell cycle or even cell death, contributing to homeostatic regulation in response to varying energy demands and stress (Quiros *et al.* 2016). In addition to mitochondrial movement along the microtubules, mitochondrial morphology can change in response to energy requirements of the cell via processes known as fusion and fission, through which mitochondria communicate within a network, and in response to intracellular stress factors causing swelling and ultimately permeability transition.

228 Mitochondria typically maintain several copies of their own genome (hundred to  
229 thousands per cell; Cummins 1998), which is maternally inherited (White *et al.* 2008) and  
230 known as mitochondrial DNA (mtDNA). One exception to strictly maternal inheritance in  
231 animals is found in bivalves (Breton *et al.* 2007). mtDNA is 16.5 kB in length, contains 13  
232 protein-coding genes for subunits of the transmembrane respiratory Complexes CI, CIII, CIV  
233 and F<sub>1</sub>F<sub>0</sub>-ATPase, and also encodes 22 tRNAs and the mitochondrial 16S and 12S rRNA.  
234 Additional gene content is encoded in the mitochondrial genome, *e.g.*, microRNAs, piRNA,  
235 smithRNAs, repeat associated RNA, and even additional proteins (Duarte *et al.* 2014; Lee *et*  
236 *al.* 2015; Cobb *et al.* 2016). The mitochondrial genome is regulated and supplemented by  
237 nuclear-encoded mitochondrial targeted proteins.

238 Abbreviation: mt, as generally used in mtDNA. Mitochondrion is singular and  
239 mitochondria is plural.

240 *‘For the physiologist, mitochondria afforded the first opportunity for an experimental*  
241 *approach to structure-function relationships, in particular those involved in active transport,*  
242 *vectorial metabolism, and metabolic control mechanisms on a subcellular level’* (Ernster and  
243 Schatz 1981).

244

245

246

247

## 1. Introduction

248

249 Mitochondria are the powerhouses of the cell with numerous physiological, molecular,  
250 and genetic functions (**Box 1**). Every study of mitochondrial function and disease is faced with  
251 **E**volution, **A**ge, **G**ender and sex, **L**ifestyle, and **E**nvironment (EAGLE) as essential background  
252 conditions intrinsic to the individual patient or subject, cohort, species, tissue and to some extent  
253 even cell line. As a large and highly coordinated group of laboratories and researchers, the  
254 mission of the global MitoEAGLE Network is to generate the necessary scale, type, and quality  
255 of consistent data sets and conditions to address this intrinsic complexity. Harmonization of  
256 experimental protocols and implementation of a quality control and data management system  
257 are required to interrelate results gathered across a spectrum of studies and to generate a  
258 rigorously monitored database focused on mitochondrial respiratory function. In this way,  
259 researchers within the same and across different disciplines will be positioned to compare  
260 findings across traditions and generations to an agreed upon set of clearly defined and accepted  
261 international standards.

262 Reliability and comparability of quantitative results depend on the accuracy of  
263 measurements under strictly-defined conditions. A conceptual framework is required to warrant  
264 meaningful interpretation and comparability of experimental outcomes carried out by research  
265 groups at different institutes. With an emphasis on quality of research, collected data can be  
266 useful far beyond the specific question of a particular experiment. Enabling meta-analytic  
267 studies is the most economic way of providing robust answers to biological questions (Cooper  
268 *et al.* 2009). Vague or ambiguous jargon can lead to confusion and may relegate valuable  
269 signals to wasteful noise. For this reason, measured values must be expressed in standardized  
270 units for each parameter used to define mitochondrial respiratory function. Standardization of  
271 nomenclature and definition of technical terms are essential to improve the awareness of the  
272 intricate meaning of current and past scientific vocabulary, for documentation and integration  
273 into databases in general, and quantitative modelling in particular (Beard 2005). The focus on  
274 coupling states and fluxes through metabolic pathways of aerobic energy transformation in  
275 mitochondrial preparations is a first step in the attempt to generate a harmonized and  
276 conceptually-oriented nomenclature in bioenergetics and mitochondrial physiology. Coupling  
277 states of intact cells, the protonmotive force, and respiratory control by fuel substrates and  
278 specific inhibitors of respiratory enzymes will be reviewed in subsequent communications.

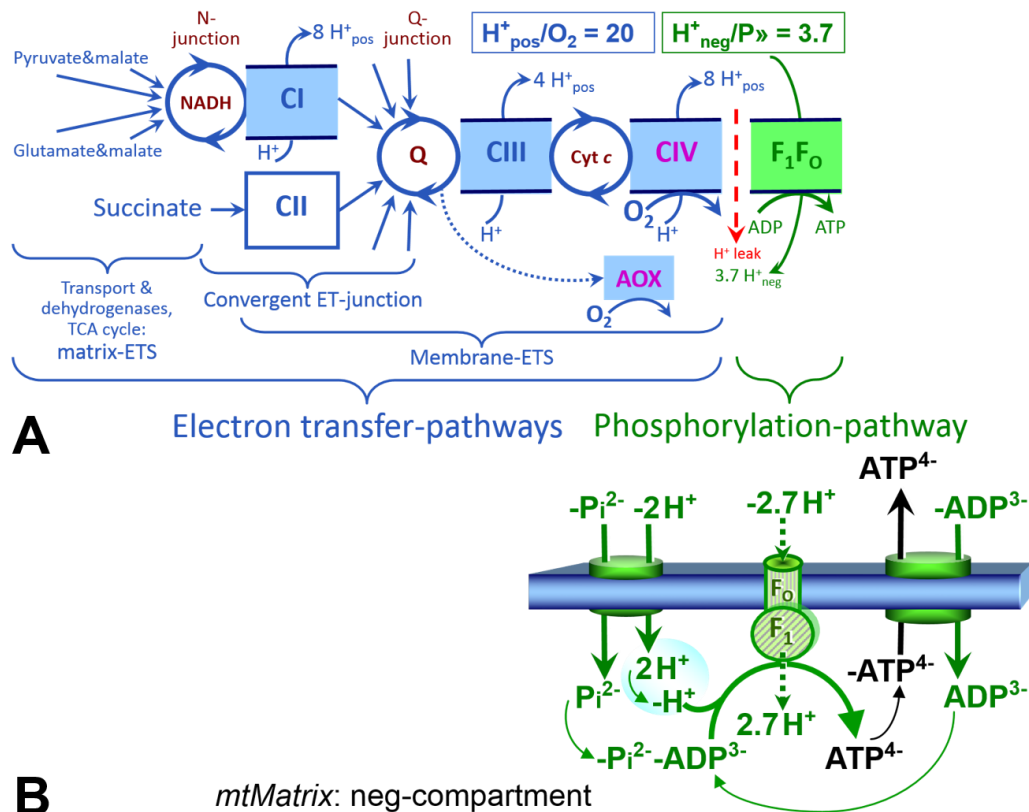
## 279 **2. Oxidative phosphorylation and coupling states in mitochondrial preparations**

280 *‘Every professional group develops its own technical jargon for talking about matters of*  
 281 *critical concern ... People who know a word can share that idea with other members of*  
 282 *their group, and a shared vocabulary is part of the glue that holds people together and*  
 283 *allows them to create a shared culture’ (Miller 1991).*

284  
 285 **Mitochondrial preparations** are defined as either isolated mitochondria, or tissue and  
 286 cellular preparations in which the barrier function of the plasma membrane is disrupted. The  
 287 plasma membrane separates the cytosol, nucleus, and organelles (the intracellular  
 288 compartment) from the environment of the cell. The plasma membrane consists of a lipid  
 289 bilayer, embedded proteins, and attached organic molecules that collectively control the  
 290 selective permeability of ions, organic molecules, and particles across the cell boundary. The  
 291 intact plasma membrane, therefore, prevents the passage of many water-soluble mitochondrial  
 292 substrates—such as succinate or adenosine diphosphate (ADP), that are required for the  
 293 analysis of respiratory capacity at kinetically-saturating concentrations; this limits the scope of  
 294 investigations into mitochondrial respiratory function in intact cells. The cholesterol content of  
 295 the plasma membrane is high compared to mitochondrial membranes. Therefore, mild  
 296 detergents—such as digitonin and saponin—can be applied to selectively permeabilize the  
 297 plasma membrane by interaction with cholesterol and allow free exchange of cytosolic  
 298 components with ions and organic molecules of the immediate cell environment, while  
 299 maintaining the integrity and localization of organelles, cytoskeleton, and the nucleus.  
 300 Application of optimum concentrations of permeabilization agents (mild detergents or toxins)  
 301 leads to the complete loss of cell viability, tested by nuclear staining and washout of cytosolic  
 302 marker enzymes—such as lactate dehydrogenase, while mitochondrial function remains intact.  
 303 The respiration rate of isolated mitochondria remains unaltered after the addition of low  
 304 concentrations of digitonin or saponin. In addition to mechanical permeabilization during  
 305 homogenization of tissue, permeabilization agents may be applied to ensure permeabilization  
 306 of all cells. Suspensions of cells permeabilized in the respiration chamber and crude tissue  
 307 homogenates contain all components of the cell at highly diluted concentrations. All  
 308 mitochondria are retained in chemically-permeabilized mitochondrial preparations and crude  
 309 tissue homogenates. In the preparation of isolated mitochondria, the cells or tissues are  
 310 homogenized, and the mitochondria are separated from other cell fractions and purified by  
 311 differential centrifugation, entailing the loss of a fraction of mitochondria. Typical  
 312 mitochondrial recovery ranges from 30% to 80%. Maximization of the purity of isolated  
 313 mitochondria may compromise not only the mitochondrial yield but also the structural and  
 314 functional integrity. Therefore, protocols to isolate mitochondria need to be optimized  
 315 according to each study. The term mitochondrial preparation does not include further  
 316 fractionation of mitochondrial components, neither submitochondrial particles.

### 317 318 *2.1. Three coupling states of mitochondrial preparations and residual oxygen consumption*

319  
 320 **Respiratory capacities in coupling control states:** To extend the classical nomenclature  
 321 on mitochondrial coupling states (Section 2.3) by a concept-driven terminology that  
 322 incorporates explicitly information on the nature of respiratory states, the terminology must be  
 323 general and not restricted to any particular experimental protocol or mitochondrial preparation  
 324 (Gnaiger 2009). We focus primarily on the conceptual ‘why’, along with clarification of the  
 325 experimental ‘how’. In the following section, the concept-driven terminology is explained and  
 326 coupling states are defined. We define respiratory capacities, comparable to channel capacity  
 327 in information theory (Schneider 2006), as the upper bound of the rate of respiration measured  
 328 in defined coupling control states and electron transfer-pathway (ET-pathway) states.



329 **Fig. 1. The oxidative phosphorylation (OXPHOS) system.** (A) The mitochondrial electron  
 330 transfer system (ETS) is fuelled by diffusion and transport of substrates across the mtOM and  
 331 mtIM and consists of the matrix-ETS and membrane-ETS. ET-pathways are coupled to the  
 332 phosphorylation-pathway. ET-pathways converge at the N-junction and Q-junction (additional  
 333 arrows indicate electron entry into the Q-junction through electron transferring flavoprotein,  
 334 glycerophosphate dehydrogenase, dihydro-orotate dehydrogenase, choline dehydrogenase, and  
 335 sulfide-ubiquinone oxidoreductase). The dotted arrow indicates the branched pathway of  
 336 oxygen consumption by alternative quinol oxidase (AOX). The  $H^+_{\text{pos}}/O_2$  ratio is the outward  
 337 proton flux from the matrix space to the positively (pos) charged compartment, divided by  
 338 catabolic  $O_2$  flux in the NADH-pathway. The  $H^+_{\text{neg}}/P$  ratio is the inward proton flux from the  
 339 inter-membrane space to the negatively (neg) charged matrix space, divided by the flux of  
 340 phosphorylation of ADP to ATP (Eq. 1). Due to ion leaks and proton slip these are not fixed  
 341 stoichiometries. (B) Phosphorylation-pathway catalyzed by the proton pump  $F_1F_0$ -ATPase,  
 342 adenine nucleotide translocase, and inorganic phosphate transporter. The  $H^+_{\text{neg}}/P$   
 343 stoichiometry is the sum of the coupling stoichiometry in the  $F_1F_0$ -ATPase reaction ( $-2.7 H^+_{\text{pos}}$   
 344 from the positive intermembrane space,  $2.7 H^+_{\text{neg}}$  to the matrix, *i.e.*, the negative compartment)  
 345 and the proton balance in the translocation of  $ADP^{2-}$ ,  $ATP^{3-}$  and  $P_i^{2-}$ . Modified from (A)  
 346 Lemieux *et al.* (2017) and (B) Gnaiger (2014).

347  
 348 To provide a diagnostic reference for respiratory capacities of core energy metabolism,  
 349 the capacity of *oxidative phosphorylation*, OXPHOS, is measured at kinetically-saturating  
 350 concentrations of ADP and inorganic phosphate,  $P_i$ . The *oxidative* ET-capacity reveals the  
 351 limitation of OXPHOS-capacity mediated by the *phosphorylation*-pathway. The ET- and  
 352 phosphorylation-pathways comprise coupled segments of the OXPHOS-system. ET-capacity  
 353 is measured as noncoupled respiration by application of *external uncouplers*. The contribution  
 354 of *intrinsically uncoupled* oxygen consumption is easily studied in the absence of ADP—by  
 355 not stimulating phosphorylation, or by inhibition of the phosphorylation-pathway. The  
 356 corresponding states are collectively classified as LEAK-states, when oxygen consumption



357 compensates mainly for ion leaks, including the proton leak (**Table 1**). Defined coupling states  
 358 are induced by: (1) adding cation chelators such as EGTA, binding free  $\text{Ca}^{2+}$  and thus limiting  
 359 cation cycling; (2) adding ADP and  $\text{P}_i$ ; (3) inhibiting the phosphorylation-pathway; and (4)  
 360 uncoupler titrations, while maintaining a defined ET-pathway state with constant fuel substrates  
 361 and inhibitors of specific branches of the ET-pathway (**Fig. 1**).  
 362

363 **Table 1. Coupling states and residual oxygen consumption in mitochondrial**  
 364 **preparations in relation to respiration- and phosphorylation-rate,  $J_{\text{kO}_2}$  and  $J_{\text{P}}$ , and**  
 365 **protonmotive force, pmf. Coupling states are established at kinetically-**  
 366 **saturating concentrations of fuel substrates and  $\text{O}_2$ .**

State	$J_{\text{kO}_2}$	$J_{\text{P}}$	pmf	Inducing factors	Limiting factors
LEAK	$L$ ; low, cation leak-dependent respiration	0	max.	proton leak, slip, and cation cycling	$J_{\text{P}} = 0$ : (1) without ADP, $L_N$ ; (2) max. ATP/ADP ratio, $L_T$ ; or (3) inhibition of the phosphorylation-pathway, $L_{\text{Omy}}$
OXPHOS	$P$ ; high, ADP-stimulated respiration	max.	high	kinetically-saturating [ADP] and [ $\text{P}_i$ ]	$J_{\text{P}}$ , by phosphorylation-pathway; or $J_{\text{kO}_2}$ by ET-capacity
ET	$E$ ; max., noncoupled respiration	0	low	optimal external uncoupler concentration for max. $J_{\text{O}_2, E}$	$J_{\text{kO}_2}$ by ET-capacity
ROX	$R_{\text{ox}}$ ; min., residual $\text{O}_2$ consumption	0	0	$J_{\text{O}_2, \text{Rox}}$ in non-ET-pathway oxidation reactions	full inhibition of ET-pathway; or absence of fuel substrates

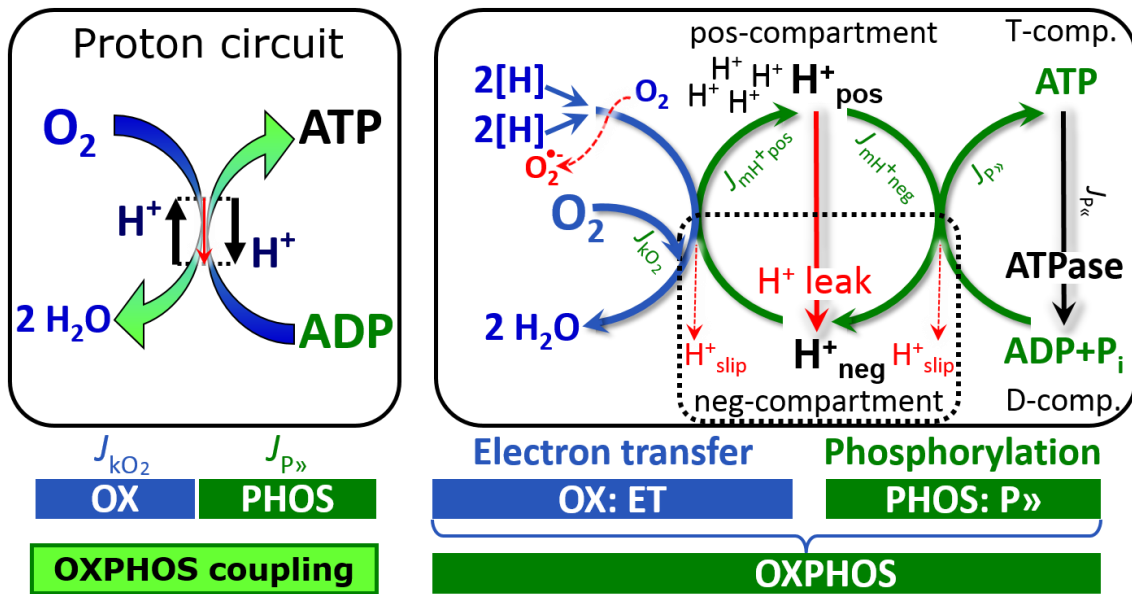
367  
 368 **Kinetic control:** Coupling control states are established in the study of mitochondrial  
 369 preparations to obtain reference values for various output variables. Physiological conditions *in*  
 370 *vivo* deviate from these experimentally obtained states. Since kinetically-saturating  
 371 concentrations, *e.g.*, of ADP or oxygen, may not apply to physiological intracellular conditions,  
 372 relevant information is obtained in studies of kinetic responses to intermediate conditions  
 373 between the LEAK state at zero [ADP] and the OXPHOS-state at saturating [ADP], or of  
 374 respiratory capacities in the range between kinetically-saturating [ $\text{O}_2$ ] and anoxia (Gnaiger  
 375 2001).

376 **The steady-state:** Mitochondria represent a thermodynamically open system in non-  
 377 equilibrium states of biochemical energy transformation. State variables (protonmotive force;  
 378 redox states) and metabolic *rates* (fluxes) are measured in defined mitochondrial respiratory  
 379 *states*. Steady states can be obtained only in open systems, in which changes by *internal*  
 380 transformations, *e.g.*,  $\text{O}_2$  consumption, are instantaneously compensated for by *external* fluxes,  
 381 *e.g.*,  $\text{O}_2$  supply, preventing a change of oxygen concentration in the system (Gnaiger 1993b).  
 382 Mitochondrial respiratory states monitored in closed systems satisfy the criteria of pseudo-  
 383 steady states for limited periods of time, when changes in the system (concentrations of  $\text{O}_2$ ,  
 384 fuel substrates, ADP,  $\text{P}_i$ ,  $\text{H}^+$ ) do not exert significant effects on metabolic fluxes (respiration,  
 385 phosphorylation). Such pseudo-steady states require respiratory media with sufficient buffering  
 386 capacity and kinetically-saturating concentrations of substrates to be maintained, and thus  
 387 depend on the kinetics of the processes under investigation.

388 **Specification of biochemical dose:** Substrates, uncouplers, inhibitors, and other  
 389 biochemical reagents are titrated to dissect mitochondrial function. Nominal concentrations of  
 390 these substances are usually reported as initial amount of substance concentration [ $\text{mol}\cdot\text{L}^{-1}$ ] in  
 391 the incubation medium. When aiming at the measurement of kinetically saturated processes—  
 392 such as OXPHOS-capacities, the concentrations for substrates can be chosen according to the  
 393 apparent equilibrium constant,  $K_m'$ . In the case of hyperbolic kinetics, only 80% of maximum  
 394 respiratory capacity is obtained at a substrate concentration of four times the  $K_m'$ , whereas  
 395 substrate concentrations of 5, 9, 19 and 49 times the  $K_m'$  are theoretically required for reaching  
 396 83%, 90%, 95% or 98% of the maximal rate (Gnaiger 2001). Other reagents are chosen to  
 397 inhibit or alter some process. The amount of these chemicals in an experimental incubation is  
 398 selected to maximize effect, yet not lead to unacceptable off-target consequences that would  
 399 adversely affect the data being sought. Specifying the amount of substance in an incubation as  
 400 nominal concentration in the aqueous incubation medium can be ambiguous (Doskey *et al.*  
 401 2015), particularly when lipophilic substances (oligomycin; uncouplers, permeabilization  
 402 agents) or cations ( $\text{TPP}^+$ ; fluorescent dyes such as safranin, TMRM) are applied which  
 403 accumulate in biological membranes or the mitochondrial matrix. For example, a dose of  
 404 digitonin of  $8 \text{ fmol}\cdot\text{cell}^{-1}$  ( $10 \mu\text{g}\cdot 10^{-6} \text{ cells}$ ) is optimal for permeabilization of endothelial cells,  
 405 and the concentration in the incubation medium has to be adjusted according to the cell density  
 406 applied (Doerrier *et al.* 2018). Generally, dose/exposure can be specified per unit of biological  
 407 sample, *i.e.*, (nominal moles of xenobiotic)/(number of cells) [ $\text{mol}\cdot\text{cell}^{-1}$ ] or, as appropriate, per  
 408 mass of biological sample [ $\text{mol}\cdot\text{kg}^{-1}$ ]. This approach to specification of dose/exposure provides  
 409 a scalable parameter that can be used to design experiments, help interpret a wide variety of  
 410 experimental results, and provide absolute information that allows researchers worldwide to  
 411 make the most use of published data (Doskey *et al.* 2015).

412 **Phosphorylation, P»:** *Phosphorylation* in the context of OXPHOS is defined as  
 413 phosphorylation of ADP by  $\text{P}_i$  to ATP. On the other hand, the term phosphorylation is used  
 414 generally in many contexts, *e.g.*, protein phosphorylation. This justifies consideration of a  
 415 symbol more discriminating and specific than P as used in the P/O ratio (phosphate to atomic  
 416 oxygen ratio;  $\text{O} = 0.5 \text{ O}_2$ ), where P indicates phosphorylation of ADP to ATP or GDP to GTP.  
 417 We propose the symbol P» for the endergonic (uphill) direction of phosphorylation  
 418  $\text{ADP}\rightarrow\text{ATP}$ , and likewise the symbol P« for the corresponding exergonic (downhill) hydrolysis  
 419  $\text{ATP}\rightarrow\text{ADP}$  (Fig. 2). P» refers mainly to electrontransfer phosphorylation but may also involve  
 420 substrate-level phosphorylation as part of the tricarboxylic acid (TCA) cycle (succinyl-CoA  
 421 ligase) and phosphorylation of ADP catalyzed by phosphoenolpyruvate carboxykinase.  
 422 Transphosphorylation is performed by adenylate kinase, creatine kinase, hexokinase and  
 423 nucleoside diphosphate kinase. In isolated mammalian mitochondria, ATP production  
 424 catalyzed by adenylate kinase ( $2 \text{ ADP} \leftrightarrow \text{ATP} + \text{AMP}$ ) proceeds without fuel substrates in the  
 425 presence of ADP (Komlódi and Tretter 2017). Kinase cycles are involved in intracellular energy  
 426 transfer and signal transduction for regulation of energy flux.

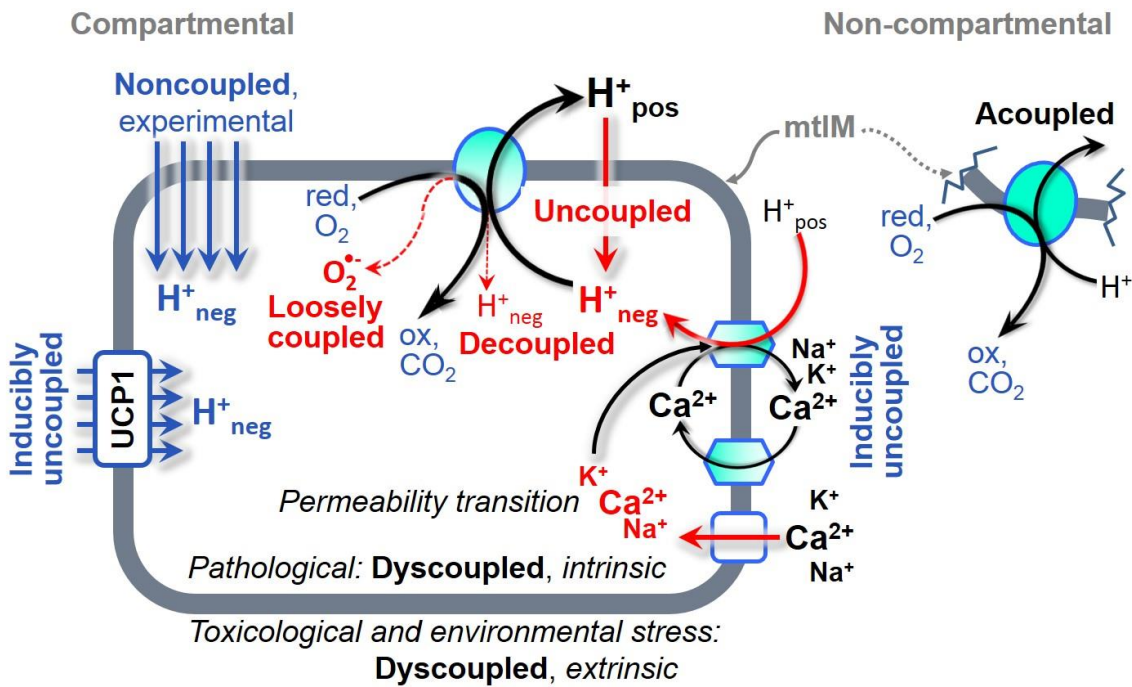
427 **Coupling:** In mitochondrial electron transfer (Fig. 1), vectorial transmembrane proton  
 428 flux is coupled through the proton pumps CI, CIII and CIV to the catabolic flux of scalar  
 429 reactions, collectively measured as oxygen flux (Fig. 2). Thus mitochondria are elements of  
 430 energy transformation. Energy cannot be lost or produced in any internal process (First Law of  
 431 thermodynamics). Open and closed systems can gain or loose energy only by external fluxes—  
 432 by exchange with the environment. Energy is a conserved quantity. Therefore, energy can  
 433 neither be produced by mitochondria, nor is there any internal process without energy  
 434 conservation. Exergy is defined as the ‘free energy’ with the potential to perform work.  
 435 *Coupling* is the mechanistic linkage of an exergonic process (spontaneous, negative exergy  
 436 change) with an endergonic process (positive exergy change) in energy transformations which  
 437 conserve part of the exergy that would be irreversible lost or dissipated in an uncoupled process.



438  
 439 **Fig. 2. The proton circuit and coupling in oxidative phosphorylation (OXPHOS).** Oxygen  
 440 flux,  $J_{kO_2}$ , through the catabolic ET-pathway,  $k$ , is coupled to flux through the phosphorylation-  
 441 pathway of ADP to ATP,  $J_{P\gg}$ . The proton pumps of the ET-pathway drive proton flux into the  
 442 positive (pos) compartment,  $J_{mH^+pos}$ , which generates the output protonmotive force (motive,  
 443 subscript  $m$ ).  $F_1F_0$ -ATPase is coupled to inward proton current into the negative (neg)  
 444 compartment,  $J_{mH^+neg}$ , to phosphorylate ADP+ $P_i$  to ATP.  $2[H]$  indicates the reduced hydrogen  
 445 equivalents of fuel substrates of the catabolic reaction  $k$  with oxygen. Fluxes are expressed per  
 446 volume,  $V$  [ $m^3$ ], of the system. The system defined by the boundaries (full black line) is not a  
 447 black box, but is analysed as a compartmental system. The negative compartment (neg-  
 448 compartment, enclosed by the dotted line) is the matrix space, separated by the mtIM from the  
 449 positive compartment (pos-compartment). ADP+ $P_i$  and ATP are the substrate- and product-  
 450 compartments (scalar ADP and ATP compartments, D-comp. and T-comp.), respectively. At  
 451 steady-state proton turnover,  $J_{\infty H^+}$ , and ATP turnover,  $J_{\infty P}$ , maintain concentrations constant,  
 452 when  $J_{mH^+\infty} = J_{mH^+pos} = J_{mH^+neg}$ , and  $J_{P\infty} = J_{P\gg} = J_{P\ll}$ . Modified from Gnaiger (2014).

453  
 454 **Uncoupling:** Uncoupling of mitochondrial respiration is a general term comprising  
 455 diverse mechanisms. Differences of terms—uncoupled vs. noncoupled—are easily overlooked,  
 456 although they relate to different mechanisms of uncoupling (Fig. 3). Rigorous definitions are  
 457 required to clarify the concepts (Table 2).

- 458  
 459  
 460  
 461  
 462  
 463  
 464  
 465
1. Proton leak across the mtIM from the pos- to the neg-compartment (Fig. 2);
  2. Cycling of other cations, strongly stimulated by permeability transition;
  3. Proton slip in the proton pumps when protons are effectively not pumped (CI, CIII and CIV) or are not driving phosphorylation ( $F_1F_0$ -ATPase);
  4. Loss of compartmental integrity when electron transfer is uncoupled;
  5. Electron leak in the loosely coupled univalent reduction of oxygen ( $O_2$ ; dioxygen) to superoxide anion radical ( $O_2^{\cdot-}$ ).



466  
467  
468  
469  
470  
471  
472  
473  
474  
475  
476

**Fig 3. Mechanisms of respiratory uncoupling.** An intact mitochondrial inner membrane, mtIM, is required for vectorial, compartmental coupling. ‘Acoupled’ respiration is the consequence of structural disruption with catalytic activity of non-compartmental mitochondrial fragments. Inducibly uncoupled (activation of UCP1) and experimentally noncoupled respiration (titration of protonophores) stimulate respiration to maximum oxygen flux of ET-capacity. Uncoupled, decoupled, and loosely coupled respiration are components of intrinsic LEAK respiration. Pathological dysfunction may affect all types of uncoupling, including permeability transition, causing intrinsically dyscoupled respiration. Similarly, toxicological and environmental stress factors can cause extrinsically dyscoupled respiration.


477  
478  
479  
480  
481  
482  
483  
484  
485  
486  
487  
488  
489  
490  
491  
492  
493  
494  
495  
496  
497  
498

**LEAK-state (Fig. 4):** The LEAK-state is defined as a state of mitochondrial respiration when  $O_2$  flux mainly compensates for ion leaks in the absence of ATP synthesis, at kinetically-saturating concentrations of  $O_2$  and respiratory fuel substrates. LEAK-respiration is measured to obtain an estimate of *intrinsic uncoupling* without addition of an experimental uncoupler: (1) in the absence of adenylates; (2) after depletion of ADP at a maximum ATP/ADP ratio; or (3) after inhibition of the phosphorylation-pathway by inhibitors of  $F_1F_0$ -ATPase—such as oligomycin, or of adenine nucleotide translocase—such as carboxyatractyloside. Adjustment of the nominal concentration of these inhibitors to the density of biological sample applied can minimize or avoid inhibitory side-effects exerted on ET-capacity or even some dyscoupling.

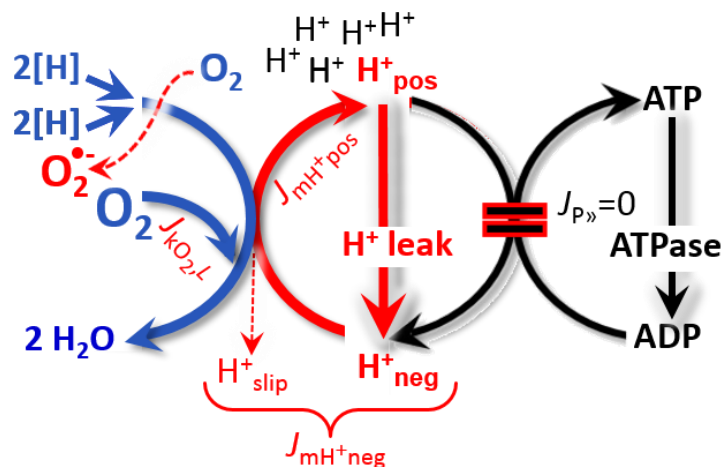


**Fig. 4. LEAK-state:** Phosphorylation is arrested,  $J_{P_{\gg}} = 0$ , and catabolic oxygen flux,  $J_{kO_2,L}$ , is controlled mainly by the proton leak,  $J_{mH^+neg,L}$ , at maximum protonmotive force. See also Fig. 2 and 3.

499 **Table 2. Distinction of terms related to respiratory coupling and uncoupling**  
 500 **(Fig. 3).**

Term	Respiration	$P \gg O_2$	Note
acoupled		0	electron transfer in mitochondrial fragments without vectorial proton translocation
uncoupled	$L$	0	non-phosphorylating intrinsic LEAK-respiration, without added protonophore
 uncoupled decoupled loosely coupled dyscoupled		0	component of LEAK-respiration, uncoupled <i>sui generis</i> , ion diffusion across the mtIM
		0	component of LEAK-respiration, proton slip
		0	component of LEAK-respiration, lower coupling due to superoxide anion radical formation and bypass of proton pumps
		0	pathologically, toxicologically, environmentally increased uncoupling, mitochondrial dysfunction
inducibly uncoupled	$E$	0	by UCP1 or cation ( <i>e.g.</i> , $Ca^{2+}$ ) cycling
noncoupled	$E$	0	non-phosphorylating respiration stimulated to maximum flux at optimum exogenous uncoupler concentration ( <b>Fig. 6</b> )
well-coupled	$P$	high	phosphorylating respiration with an intrinsic LEAK component ( <b>Fig. 5</b> )
fully coupled	$P - L$	max.	OXPHOS-capacity corrected for LEAK-respiration ( <b>Fig. 7</b> )

501  
 502 **Proton leak and uncoupled respiration:** Proton leak is a leak current of protons. The  
 503 intrinsic proton leak is the *uncoupled* process in which protons diffuse across the mtIM in the  
 504 dissipative direction of the downhill protonmotive force without coupling to phosphorylation  
 505 (**Fig. 4**). The proton leak flux depends non-linearly on the protonmotive force (Garlid *et al.*  
 506 1989; Divakaruni and Brand 2011), it is a property of the mtIM and may be enhanced due to  
 507 possible contaminations by free fatty acids. Inducible uncoupling mediated by uncoupling  
 508 protein 1 (UCP1) is physiologically controlled, *e.g.*, in brown adipose tissue. UCP1 is a member  
 509 of the mitochondrial carrier family which is involved in the translocation of protons across the  
 510 mtIM (Klingenberg 2017). Consequently, the short-circuit diminishes the protonmotive force  
 511 and stimulates electron transfer to  $O_2$  and heat dissipation without phosphorylation of ADP.

512 **Cation cycling:** There can be other cation contributors to leak current including calcium  
 513 and probably magnesium. Calcium current is balanced by mitochondrial  $Na^+/Ca^{2+}$  exchange,  
 514 which is balanced by  $Na^+/H^+$  or  $K^+/H^+$  exchanges. This is another effective uncoupling  
 515 mechanism different from proton leak.

516 **Proton slip and decoupled respiration:** Proton slip is the *decoupled* process in which  
 517 protons are only partially translocated by a proton pump of the ET-pathways and slip back to  
 518 the original compartment. The proton leak is the dominant contributor to the overall leak current  
 519 in mammalian mitochondria incubated under physiological conditions at 37 °C, whereas proton  
 520 slip is increased at lower experimental temperature (Canton *et al.* 1995). Proton slip can also  
 521 happen in association with the  $F_1F_0$ -ATPase, in which the proton slips downhill across the  
 522 pump to the matrix without contributing to ATP synthesis. In each case, proton slip is a property  
 523 of the proton pump and increases with the pump turnover rate.

524 **Electron leak and loosely coupled respiration:** The production of superoxide anion  
 525 radical by the ETS leads to a bypass of proton pumps and correspondingly lower  $P_{\gg}/O_2$  ratio.  
 526 This depends on the actual site of electron leak and the scavenging of hydrogen peroxide by  
 527 cytochrome *c*, whereby electrons may re-enter the ETS with proton translocation by CIV.

528 **Loss of compartmental integrity and acoupled respiration:** Electron transfer and  $O_2$   
 529 consumption proceed without compartmental proton translocation in disrupted mitochondrial  
 530 fragments. Such fragments form during mitochondrial isolation, and may not fully fuse to re-  
 531 establish structurally intact mitochondria. Loss of mtIM integrity, therefore, is the cause of  
 532 acoupled respiration, which is a nonvectorial dissipative process without control by the  
 533 protonmotive force.

534 **Dyscoupled respiration:** Mitochondrial injuries may lead to *dyscoupling* as a  
 535 pathological or toxicological cause of *uncoupled* respiration. Dyscoupling may involve any  
 536 type of uncoupling mechanism, *e.g.*, opening the permeability transition pore. Dyscoupled  
 537 respiration is distinguished from the experimentally induced *noncoupled* respiration in the ET-  
 538 state (**Fig. 3**).

539  
 540 **OXPHOS-state (Fig. 5):**

541 The OXPHOS-state is defined as  
 542 the respiratory state with  
 543 kinetically-saturating  
 544 concentrations of  $O_2$ , respiratory  
 545 and phosphorylation substrates,  
 546 and absence of exogenous  
 547 uncoupler, which provides an  
 548 estimate of the maximal  
 549 respiratory capacity in the  
 550 OXPHOS-state for any given ET-  
 551 pathway state. Respiratory  
 552 capacities at kinetically-saturating  
 553 substrate concentrations provide  
 554 reference values or upper limits of  
 555 performance, aiming at the  
 556 generation of data sets for  
 557 comparative purposes. Physiological activities and effects of substrate kinetics can be evaluated  
 558 relative to the OXPHOS-capacity.

559 As discussed previously, 0.2 mM ADP does not fully saturate flux in isolated  
 560 mitochondria (Gnaiger 2001; Puchowicz *et al.* 2004); greater ADP concentration is required,  
 561 particularly in permeabilized muscle fibres and cardiomyocytes, to overcome limitations by  
 562 intracellular diffusion and by the reduced conductance of the mtOM (Jepihhina *et al.* 2011,  
 563 Illaste *et al.* 2012, Simson *et al.* 2016), either through interaction with tubulin (Rostovtseva *et al.*  
 564 2008) or other intracellular structures (Birkedal *et al.* 2014). In permeabilized muscle fibre  
 565 bundles of high respiratory capacity, the apparent  $K_m$  for ADP increases up to 0.5 mM (Saks *et al.*  
 566 1998), consistent with experimental evidence that >90% saturation is reached only at >5  
 567 mM ADP (Pesta and Gnaiger 2012). Similar ADP concentrations are also required for accurate  
 568 determination of OXPHOS-capacity in human clinical cancer samples and permeabilized cells  
 569 (Klepinin *et al.* 2016; Koit *et al.* 2017). Whereas 2.5 to 5 mM ADP is sufficient to obtain the  
 570 actual OXPHOS-capacity in many types of permeabilized tissue and cell preparations,  
 571 experimental validation is required in each specific case.

572

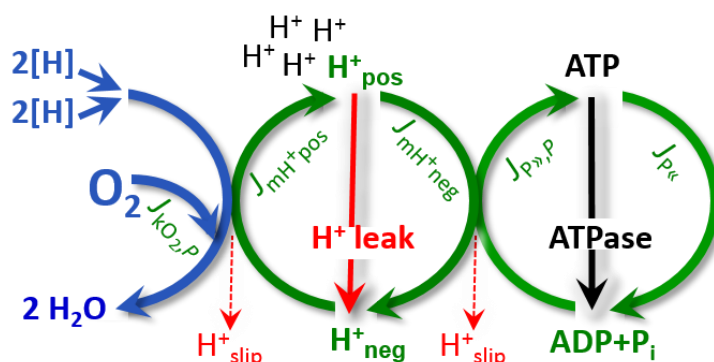
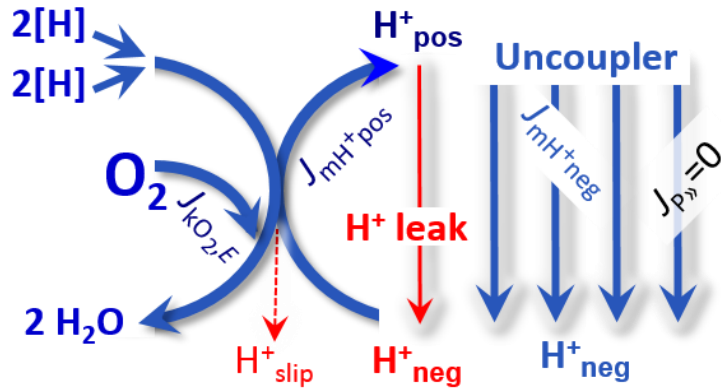


**Fig. 5. OXPHOS-state:** Phosphorylation,  $J_{P_{\gg}}$ , is stimulated by kinetically-saturating [ADP] and inorganic phosphate, [P<sub>i</sub>], and is supported by a high protonmotive force.  $O_2$  flux,  $J_{kO_2,P}$ , is well-coupled at a  $P_{\gg}/O_2$  ratio of  $J_{P_{\gg},P}/J_{kO_2,P}$ . See also **Fig. 2**.

573 **Electron transfer-state**  
 574 (Fig. 6): The ET-state is defined  
 575 as the *noncoupled* state with  
 576 kinetically-saturating  
 577 concentrations of O<sub>2</sub>, respiratory  
 578 substrate and optimum  
 579 *exogenous* uncoupler  
 580 concentration for maximum O<sub>2</sub>  
 581 flux, as an estimate of ET-  
 582 capacity. Inhibition of  
 583 respiration is observed at higher  
 584 than optimum uncoupler  
 585 concentrations. As a consequence  
 586 of the nearly collapsed  
 587 protonmotive force, the driving  
 588 force is insufficient for  
 589 phosphorylation, and  $J_{P_{\gg}} = 0$ .



590  
 591  
 592  
 593  
 594  
 595  
 596  
 597  
 598  
 599  
 600  
 601  
 602  
 603  
 604  
 605  
 606  
 607  
 608  
 609  
 610  
 611  
 612  
 613  
 614  
 615  
 616  
 617  
 618  
 619

**Fig. 6. ET-state:** Noncoupled respiration,  $J_{kO_2,E}$ , is maximum at optimum exogenous uncoupler concentration and phosphorylation is zero,  $J_{P_{\gg}} = 0$ . See also Fig. 2.

Besides the three fundamental coupling states of mitochondrial preparations, the following respiratory state is relevant to assess respiratory function:

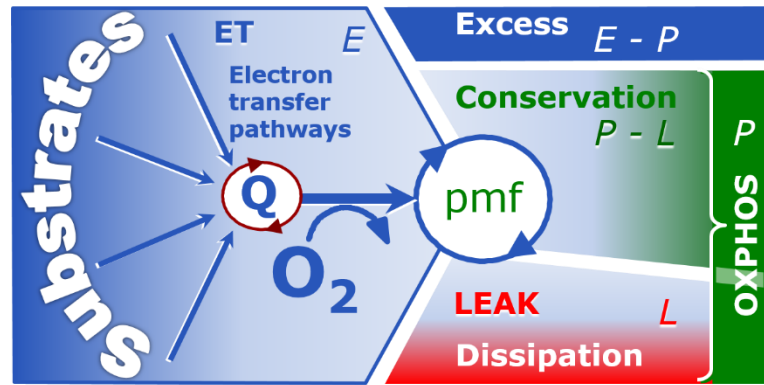
**ROX state and *Rox*:** The rate of residual oxygen consumption, *Rox*, is defined as O<sub>2</sub> consumption due to oxidative side reactions remaining after inhibition of ET—with rotenone, malonic acid and antimycin A. Cyanide and azide not only inhibit CIV but also several peroxidases involved in *Rox*. ROX is not a coupling state. *Rox* represents a baseline that is used to correct mitochondrial respiration in defined coupling states. *Rox* is not necessarily equivalent to non-mitochondrial respiration, considering oxygen-consuming reactions in mitochondria not related to ET—such as oxygen consumption in reactions catalyzed by monoamine oxidases (type A and B), monooxygenases (cytochrome P450 monooxygenases), dioxygenase (sulfur dioxygenase and trimethyllysine dioxygenase), and several hydroxylases. Mitochondrial preparations, especially those obtained from liver, may be contaminated by peroxisomes. This fact makes the exact determination of mitochondrial oxygen consumption and mitochondria-associated generation of reactive oxygen species complicated (Schönfeld *et al.* 2009). The dependence of ROX-linked oxygen consumption needs to be studied in detail together with non-ET enzyme activities, availability of specific substrates, oxygen concentration, and electron leakage leading to the formation of reactive oxygen species.

## 2.2. Coupling states and respiratory rates

As an improvement of previous terminologies, we distinguish metabolic *pathways* from metabolic *states* and the corresponding metabolic *rates*; for example: ET-pathways (Fig. 7), ET-state (Fig. 6), and ET-capacity, *E*, respectively (Table 1). The protonmotive force is *high* in the OXPHOS-state when it drives phosphorylation, *maximum* in the LEAK-state of coupled mitochondria, driven by LEAK-respiration at a minimum back flux of cations to the matrix side, and *very low* in the ET-state when uncouplers short-circuit the proton cycle (Table 1).

The three coupling states, ET, LEAK and OXPHOS, are shown schematically with the corresponding respiratory rates, abbreviated as *E*, *L* and *P*, respectively (Fig. 7).

620 **Fig. 7. Four-compartment**  
 621 **model of oxidative**  
 622 **phosphorylation.** Respiratory  
 623 states (ET, OXPHOS, LEAK)  
 624 and corresponding rates ( $E$ ,  $P$ ,  $L$ )  
 625 are connected by the  
 626 protonmotive force, pmf.  
 627 Electron transfer-capacity,  $E$ , is  
 628 partitioned into (1) dissipative  
 629 LEAK-respiration,  $L$ , when the  
 630 Gibbs energy change of catabolic  
 631  $O_2$  consumption is irreversibly lost, (2) net OXPHOS-capacity,  $P-L$ , with partial conservation  
 632 of the capacity to perform work, and (3) the excess capacity,  $E-P$ . Modified from Gnaiger  
 633 (2014).



634  
 635  $E$  may exceed or be equal to  $P$ .  $E > P$  is observed in many types of mitochondria, varying  
 636 between species, tissues and cell types (Gnaiger 2009).  $E-P$  is the excess ET-capacity pushing  
 637 the phosphorylation-flux (**Fig. 1B**) to the limit of its *capacity of utilizing* the protonmotive force.  
 638 In addition, the magnitude of  $E-P$  depends on the tightness of respiratory coupling or degree of  
 639 uncoupling, since an increase of  $L$  causes  $P$  to increase towards the limit of  $E$ . The *excess*  $E-P$   
 640 capacity,  $E-P$ , therefore, provides a sensitive diagnostic indicator of specific injuries of the  
 641 phosphorylation-pathway, under conditions when  $E$  remains constant but  $P$  declines relative to  
 642 controls (**Fig. 7**). Substrate cocktails supporting simultaneous convergent electron transfer to  
 643 the Q-junction for reconstitution of TCA cycle function establish pathway control states with  
 644 high ET-capacity, and consequently increase the sensitivity of the  $E-P$  assay.

645  $E$  cannot theoretically be lower than  $P$ .  $E < P$  must be discounted as an artefact, which  
 646 may be caused experimentally by: (1) loss of oxidative capacity during the time course of the  
 647 respirometric assay, since  $E$  is measured subsequently to  $P$ ; (2) using insufficient uncoupler  
 648 concentrations; (3) using high uncoupler concentrations which inhibit ET (Gnaiger 2008); (4)  
 649 high oligomycin concentrations applied for measurement of  $L$  before titrations of uncoupler,  
 650 when oligomycin exerts an inhibitory effect on  $E$ . On the other hand, the excess ET-capacity is  
 651 overestimated if non-saturating  $[ADP]$  or  $[P_i]$  are used. See State 3 in the next section.

652  **$P_{\gg}/O_2$  ratio:** The  $P_{\gg}/O_2$  ratio ( $P_{\gg}/4 e^-$ ) is two times the 'P/O' ratio ( $P_{\gg}/2 e^-$ ) of classical  
 653 bioenergetics.  $P_{\gg}/O_2$  is a generalized symbol, independent phosphorylation assessment by  
 654 determination of  $P_i$  consumption ( $P_i/O_2$  flux ratio), ADP depletion ( $ADP/O_2$  flux ratio), or ATP  
 655 production ( $ATP/O_2$  flux ratio).

656 The mechanistic  $P_{\gg}/O_2$  ratio—or  $P_{\gg}/O_2$  stoichiometry—is calculated from the proton-to-  
 657 oxygen and proton-to-phosphorylation coupling stoichiometries (**Fig. 1A**),  
 658

$$659 \quad P_{\gg}/O_2 = \frac{H_{pos}^+/O_2}{H_{neg}^+/P_{\gg}} \quad (1)$$

660  
 661 The  $H_{pos}^+/O_2$  *coupling stoichiometry* (referring to the full 4 electron reduction of  $O_2$ ) depends  
 662 on the ET-pathway control state which defines the relative involvement of the three coupling  
 663 sites (CI, CIII and CIV) in the catabolic pathway of electrons to  $O_2$ . This varies with: (1) a  
 664 bypass of CI by single or multiple electron input into the Q-junction; and (2) a bypass of CIV  
 665 by involvement of AOX.  $H_{pos}^+/O_2$  is 12 in the ET-pathways involving CIII and CIV as proton  
 666 pumps, increasing to 20 for the NADH-pathway (**Fig. 1A**), but a general consensus on  $H_{pos}^+/O_2$   
 667 stoichiometries remains to be reached (Hinkle 2005; Wikström and Hummer 2012; Sazanov  
 668 2015). The  $H_{neg}^+/P_{\gg}$  coupling stoichiometry (3.7; **Fig. 1A**) is the sum of 2.7  $H_{neg}^+$  required by  
 669 the  $F_1F_0$ -ATPase of vertebrate and most invertebrate species (Watt *et al.* 2010) and the proton



670 balance in the translocation of ADP, ATP and  $P_i$  (**Fig. 1B**). Taken together, the mechanistic  
 671  $P_{\gg}/O_2$  ratio is calculated at 5.4 and 3.3 for NADH- and succinate-linked respiration, respectively  
 672 (Eq. 1). The corresponding classical  $P_{\gg}/O$  ratios (referring to the 2 electron reduction of  $0.5 O_2$ )  
 673 are 2.7 and 1.6 (Watt *et al.* 2010), in direct agreement with the measured  $P_{\gg}/O$  ratio for succinate  
 674 of  $1.58 \pm 0.02$  (Gnaiger *et al.* 2000).

675 The effective  $P_{\gg}/O_2$  flux ratio ( $Y_{P_{\gg}/O_2} = J_{P_{\gg}}/J_{kO_2}$ ) is diminished relative to the mechanistic  
 676  $P_{\gg}/O_2$  ratio by intrinsic and extrinsic uncoupling and dyscoupling (**Fig. 3**). Such generalized  
 677 uncoupling is different from switching to mitochondrial pathways that involve fewer than three  
 678 proton pumps ('coupling sites': Complexes CI, CIII and CIV), bypassing CI through multiple  
 679 electron entries into the Q-junction, or CIII and CIV through AOX (**Fig. 1**). Reprogramming of  
 680 mitochondrial pathways may be considered as a switch of gears (changing the stoichiometry)  
 681 rather than uncoupling (loosening the stoichiometry). In addition,  $Y_{P_{\gg}/O_2}$  depends on several  
 682 experimental conditions of flux control, increasing as a hyperbolic function of [ADP] to a  
 683 maximum value (Gnaiger 2001).

684 The net OXPHOS-capacity is calculated by subtracting  $L$  from  $P$  (**Fig. 7**). Then the net  
 685  $P_{\gg}/O_2$  equals  $P_{\gg}/(P-L)$ , wherein the dissipative LEAK component in the OXPHOS-state may  
 686 be overestimated. This can be avoided by measuring LEAK-respiration in a state when the  
 687 protonmotive force is adjusted to its slightly lower value in the OXPHOS-state—by titration of  
 688 an ET inhibitor (Divakaruni and Brand 2011). Any turnover-dependent components of proton  
 689 leak and slip, however, are underestimated under these conditions (Garlid *et al.* 1993). In  
 690 general, it is inappropriate to use the term *ATP production* or *ATP turnover* for the difference  
 691 of oxygen consumption measured in states  $P$  and  $L$ . The difference  $P-L$  is the upper limit of the  
 692 part of OXPHOS-capacity that is freely available for ATP production (corrected for LEAK-  
 693 respiration) and is fully coupled to phosphorylation with a maximum mechanistic stoichiometry  
 694 (**Fig. 7**).

695 **Control and regulation:** The terms metabolic *control* and *regulation* are frequently used  
 696 synonymously, but are distinguished in metabolic control analysis: 'We could understand the  
 697 regulation as the mechanism that occurs when a system maintains some variable constant over  
 698 time, in spite of fluctuations in external conditions (homeostasis of the internal state). On the  
 699 other hand, metabolic control is the power to change the state of the metabolism in response to  
 700 an external signal' (Fell 1997). Respiratory control may be induced by experimental control  
 701 signals that *exert* an influence on: (1) ATP demand and ADP phosphorylation-rate; (2) fuel  
 702 substrate composition, pathway competition; (3) available amounts of substrates and oxygen,  
 703 *e.g.*, starvation and hypoxia; (4) the protonmotive force, redox states, flux–force relationships,  
 704 coupling and efficiency; (5)  $Ca^{2+}$  and other ions including  $H^+$ ; (6) inhibitors, *e.g.*, nitric oxide  
 705 or intermediary metabolites such as oxaloacetate; (7) signalling pathways and regulatory  
 706 proteins, *e.g.*, insulin resistance, transcription factor hypoxia inducible factor 1. *Mechanisms* of  
 707 respiratory control and regulation include adjustments of: (1) enzyme activities by allosteric  
 708 mechanisms and phosphorylation; (2) enzyme content, concentrations of cofactors and  
 709 conserved moieties—such as adenylates, nicotinamide adenine dinucleotide [ $NAD^+/NADH$ ],  
 710 coenzyme Q, cytochrome *c*); (3) metabolic channeling by supercomplexes; and (4)  
 711 mitochondrial density (enzyme concentrations and membrane area) and morphology (cristae  
 712 folding, fission and fusion). Mitochondria are targeted directly by hormones, thereby affecting  
 713 their energy metabolism (Lee *et al.* 2013; Gerö and Szabo 2016; Price and Dai 2016; Moreno  
 714 *et al.* 2017). Evolutionary or acquired differences in the genetic and epigenetic basis of  
 715 mitochondrial function (or dysfunction) between subjects and gene therapy; age; gender,  
 716 biological sex, and hormone concentrations; life style including exercise and nutrition; and  
 717 environmental issues including thermal, atmospheric, toxicological and pharmacological  
 718 factors, exert an influence on all control mechanisms listed above. For reviews, see Brown  
 719 1992; Gnaiger 1993a, 2009; 2014; Paradies *et al.* 2014; Morrow *et al.* 2017.

720 **Respiratory control and response:** Lack of control by a metabolic pathway, *e.g.*,  
 721 phosphorylation-pathway, means that there will be no response to a variable activating it, *e.g.*,  
 722 [ADP]. The reverse, however, is not true as the absence of a response to [ADP] does not exclude  
 723 the phosphorylation-pathway from having some degree of control. The degree of control of a  
 724 component of the OXPHOS-pathway on an output variable—such as oxygen flux, will in  
 725 general be different from the degree of control on other outputs—such as phosphorylation-flux  
 726 or proton leak flux. Therefore, it is necessary to be specific as to which input and output are  
 727 under consideration (Fell 1997).

728 **Respiratory coupling control:** Respiratory control refers to the ability of mitochondria  
 729 to adjust oxygen consumption in response to external control signals by engaging various  
 730 mechanisms of control and regulation. Respiratory control is monitored in a mitochondrial  
 731 preparation under conditions defined as respiratory states. When phosphorylation of ADP to  
 732 ATP is stimulated or depressed, an increase or decrease is observed in electron flux linked to  
 733 oxygen consumption in respiratory coupling states of intact mitochondria ('controlled states' in  
 734 the classical terminology of bioenergetics). Alternatively, coupling of electron transfer with  
 735 phosphorylation is disengaged by disruption of the integrity of the mtIM or by uncouplers,  
 736 functioning like a clutch in a mechanical system. The corresponding coupling control state is  
 737 characterized by high levels of oxygen consumption without control by phosphorylation  
 738 ('uncontrolled state').

739 **ET-pathway control states** are obtained in mitochondrial preparations by depletion of  
 740 endogenous substrates and addition to the mitochondrial respiration medium of fuel substrates  
 741 (CHNO; 2[H]) and specific inhibitors, activating selected mitochondrial catabolic pathways, *k*  
 742 (**Fig. 1 and 2**). Coupling control states and pathway control states are complementary, since  
 743 mitochondrial preparations depend on an exogenous supply of pathway-specific fuel substrates  
 744 and oxygen (Gnaiger 2014).

### 745 2.3. Classical terminology for isolated mitochondria

746 *'When a code is familiar enough, it ceases appearing like a code; one forgets that there*  
 747 *is a decoding mechanism. The message is identical with its meaning' (Hofstadter 1979).*

750 Chance and Williams (1955; 1956) introduced five classical states of mitochondrial respiration  
 751 and cytochrome redox states. **Table 3** shows a protocol with isolated mitochondria in a closed  
 752 respirometric chamber, defining a sequence of respiratory states. States and rates are not  
 753 specifically distinguished in this nomenclature.

754  
 755 **Table 3. Metabolic states of mitochondria (Chance and**  
 756 **Williams, 1956; Table V).**

State	[O <sub>2</sub> ]	ADP level	Substrate Level	Respiration rate	Rate-limiting substance
1	>0	low	low	slow	ADP
2	>0	high	~0	slow	substrate
3	>0	high	high	fast	respiratory chain
4	>0	low	high	slow	ADP
5	0	high	high	0	oxygen

758

759

760 **State 1** is obtained after addition of isolated mitochondria to air-saturated  
 761 isoosmotic/isotonic respiration medium containing inorganic phosphate, but no fuel substrates  
 762 and no adenylates, *i.e.*, AMP, ADP, ATP.

763 **State 2** is induced by addition of a ‘high’ concentration of ADP (typically 100 to 300  
 764  $\mu\text{M}$ ), which stimulates respiration transiently on the basis of endogenous fuel substrates and  
 765 phosphorylates only a small portion of the added ADP. State 2 is then obtained at a low  
 766 respiratory activity limited by exhausted endogenous fuel substrate availability (**Table 3**). If  
 767 addition of specific inhibitors of respiratory complexes—such as rotenone—does not cause a  
 768 further decline of oxygen consumption, State 2 is equivalent to the state of residual oxygen  
 769 consumption, ROX (See below.). If inhibition is observed, undefined endogenous fuel  
 770 substrates are a confounding factor of pathway control, contributing to the effect of  
 771 subsequently externally added substrates and inhibitors. In contrast to the original protocol, an  
 772 alternative sequence of titration steps is frequently applied, in which the alternative ‘State 2’  
 773 has an entirely different meaning, when this second state is induced by addition of fuel substrate  
 774 without ADP (LEAK-state; in contrast to State 2 defined in **Table 1** as a ROX state), followed  
 775 by addition of ADP.

776 **State 3** is the state stimulated by addition of fuel substrates while the ADP concentration  
 777 is still high (**Table 3**) and supports coupled energy transformation through oxidative  
 778 phosphorylation. ‘High ADP’ is a concentration of ADP specifically selected to allow the  
 779 measurement of State 3 to State 4 transitions of isolated mitochondria in a closed respirometric  
 780 chamber. Repeated ADP titration re-establishes State 3 at ‘high ADP’. Starting at oxygen  
 781 concentrations near air-saturation (ca. 200  $\mu\text{M}$   $\text{O}_2$  at sea level and 37 °C), the total ADP  
 782 concentration added must be low enough (typically 100 to 300  $\mu\text{M}$ ) to allow phosphorylation  
 783 to ATP at a coupled rate of oxygen consumption that does not lead to oxygen depletion during  
 784 the transition to State 4. In contrast, kinetically-saturating ADP concentrations usually are 10-  
 785 fold higher than ‘high ADP’, e.g., 2.5 mM in isolated mitochondria. The abbreviation State 3u  
 786 is occasionally used in bioenergetics, to indicate the state of respiration after titration of an  
 787 uncoupler, without sufficient emphasis on the fundamental difference between OXPHOS-  
 788 capacity (*well-coupled* with an *endogenous* uncoupled component) and ET-capacity  
 789 (*noncoupled*).

790 **State 4** is a LEAK-state that is obtained only if the mitochondrial preparation is intact  
 791 and well-coupled. Depletion of ADP by phosphorylation to ATP leads to a decline in the rate  
 792 of oxygen consumption in the transition from State 3 to State 4. Under these conditions of State  
 793 4, a maximum protonmotive force and high ATP/ADP ratio are maintained. For calculation of  
 794  $P_{\gg}/\text{O}_2$  ratios the gradual decline of  $Y_{P_{\gg}/\text{O}_2}$  towards diminishing [ADP] at State 4 must be taken  
 795 into account (Gnaiger 2001). State 4 respiration,  $L_T$  (**Table 1**), reflects intrinsic proton leak and  
 796 intrinsic ATP hydrolysis activity. Oxygen consumption in State 4 is an overestimation of  
 797 LEAK-respiration if the contaminating ATP hydrolysis activity recycles some ATP to ADP,  
 798  $J_{P_{\ll}}$ , which stimulates respiration coupled to phosphorylation,  $J_{P_{\gg}} > 0$ . This can be tested by  
 799 inhibition of the phosphorylation-pathway using oligomycin, ensuring that  $J_{P_{\gg}} = 0$  (State 4o).  
 800 Alternatively, sequential ADP titrations re-establish State 3, followed by State 3 to State 4  
 801 transitions while sufficient oxygen is available. Anoxia may be reached, however, before  
 802 exhaustion of ADP (State 5).

803 **State 5** is the state after exhaustion of oxygen in a closed respirometric chamber.  
 804 Diffusion of oxygen from the surroundings into the aqueous solution may be a confounding  
 805 factor preventing complete anoxia (Gnaiger 2001). Chance and Williams (1955) provide an  
 806 alternative definition of State 5, which gives it the different meaning of ROX versus anoxia:  
 807 ‘State 5 may be obtained by antimycin A treatment or by anaerobiosis’.

808 In **Table 3**, only States 3 and 4 (and ‘State 2’ in the alternative protocol: addition of fuel  
 809 substrates without ADP; not included in the table) are coupling control states, with the  
 810 restriction that  $\text{O}_2$  flux in State 3 may be limited kinetically by non-saturating ADP  
 811 concentrations (**Table 1**).

812  
 813

### 814 3. Normalization: fluxes and flows

815

#### 816 3.1. Normalization: system or sample

817

818 The term *rate* is not sufficiently defined to be useful for a database (Fig. 8). The  
 819 inconsistency of the meanings of rate becomes fully apparent when considering Galileo  
 820 Galilei's famous principle, that 'bodies of different weight all fall at the same rate (have a  
 821 constant acceleration)' (Coopersmith 2010).

822

823 **Fig. 8. Different meanings of**  
 824 **rate may lead to confusion, if**  
 825 **the normalization is not**  
 826 **sufficiently specified.** Results are  
 827 frequently expressed as mass-  
 828 specific *flux*,  $J_{mX}$ , per mg protein,  
 829 dry or wet weight (mass). Cell  
 830 volume,  $V_{\text{cell}}$ , may be used for  
 831 normalization (volume-specific  
 832 flux,  $J_{V\text{cell}}$ ), which must be clearly  
 833 distinguished from flow per cell,  
 834  $I_{N\text{cell}}$ , or flux,  $J_V$ , expressed for  
 835 methodological reasons per  
 836 volume of the measurement  
 837 system. For details see Table 4.

838

839 **Flow per system,  $I$ :** In a generalization of electrical terms, flow as an extensive quantity  
 840 (per system) is distinguished from flux as a size-specific quantity (per system size) (Fig. 8).  
 841 Electric current is flow,  $I_{\text{el}}$  [ $\text{A} \equiv \text{C}\cdot\text{s}^{-1}$ ] per system (extensive quantity). When dividing this  
 842 extensive quantity by system size (cross-sectional area of a 'wire'), a size-specific quantity is  
 843 obtained, which is flux (current density),  $J_{\text{el}}$  [ $\text{A}\cdot\text{m}^{-2} = \text{C}\cdot\text{s}^{-1}\cdot\text{m}^{-2}$ ].

844 **Extensive quantities:** An extensive quantity increases proportionally with system size.  
 845 The magnitude of an extensive quantity is completely additive for non-interacting  
 846 subsystems—such as mass or flow expressed per defined system. The magnitude of these  
 847 quantities depends on the extent or size of the system (Cohen *et al.* 2008).

848 **Size-specific quantities:** 'The adjective *specific* before the name of an extensive quantity  
 849 is often used to mean *divided by mass*' (Cohen *et al.* 2008). In this system-paradigm, mass-  
 850 specific flux is flow divided by mass of the *system* (the total mass of everything within the  
 851 measuring chamber). A mass-specific quantity is independent of the extent of non-interacting  
 852 homogenous subsystems. Tissue-specific quantities (related to the *sample* in contrast to the  
 853 *system*) are of fundamental interest in comparative mitochondrial physiology, where *specific*  
 854 refers to the *type of the sample* rather than *mass of the system*. The term *specific*, therefore, must  
 855 be clarified; *sample-specific*, e.g., muscle mass-specific normalization, is distinguished from  
 856 *system-specific* (mass or volume) quantities (Fig. 8).

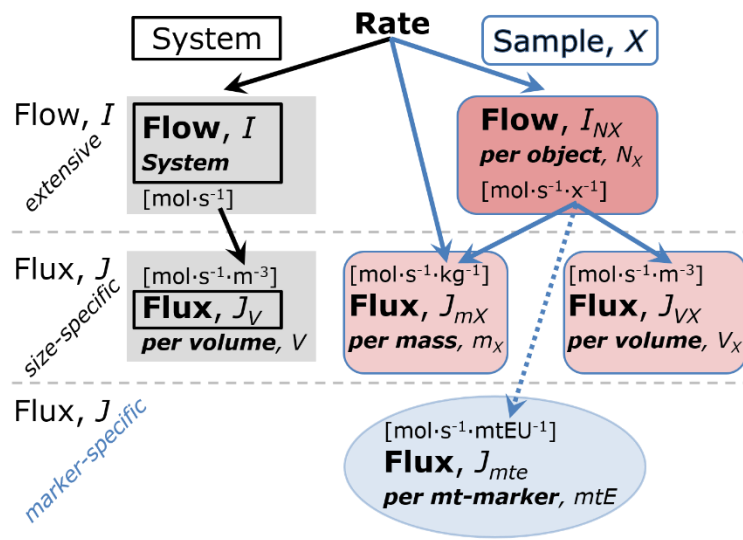
857

---

#### 858 **Box 2: Metabolic fluxes and flows: vectorial and scalar**

859

860 Fluxes are *vectors*, if they have *spatial* direction in addition to magnitude. A vector flux  
 861 (surface-density of flow) is expressed per unit cross-sectional area,  $A$  [ $\text{m}^2$ ], perpendicular to the  
 862 direction of flux. *Flows* are defined as extensive quantities of the *system*, as vector or scalar  
 863 flow,  $I$  or  $I$  [ $\text{mol}\cdot\text{s}^{-1}$ ], respectively, then the corresponding vector and scalar *fluxes* are  $J = I\cdot A^{-1}$   
 864 [ $\text{mol}\cdot\text{s}^{-1}\cdot\text{m}^{-2}$ ] and  $J = I\cdot V^{-1}$  [ $\text{mol}\cdot\text{s}^{-1}\cdot\text{m}^{-3}$ ], respectively, expressing flux as an area-specific vector



865 or volume-specific scalar quantity. We suggest to define: (1) *vectoral* fluxes, which analyze  
 866 translocations in continuous systems as functions of gradients; (2) *vectorial* fluxes, which  
 867 describe translocations in discontinuous systems and are restricted to information on  
 868 compartmental differences (**Fig. 2**, transmembrane proton flux); and (3) *scalar* fluxes, which  
 869 are transformations in a homogenous system (**Fig. 2**, catabolic O<sub>2</sub> flux,  $J_{kO_2}$  [mol·s<sup>-1</sup>·m<sup>-3</sup>]).

870 Vectorial transmembrane proton fluxes,  $J_{mH^+pos}$  and  $J_{mH^+neg}$ , are analyzed in a  
 871 heterogenous compartmental system as a quantity with *directional* but not *spatial* information.  
 872 Translocation of protons across the mtIM has a defined direction, either from the negative  
 873 compartment (matrix space; negative, neg-compartment) to the positive compartment (inter-  
 874 membrane space; positive, pos-compartment) or *vice versa* (**Fig. 2**). The arrows defining the  
 875 direction of the translocation between the two compartments may point upwards or downwards,  
 876 right or left, without any implication that these are actual directions in space. The pos-  
 877 compartment is neither above nor below the neg-compartment in a spatial sense, but can be  
 878 visualized arbitrarily in a figure in the upper position (**Fig. 2**). In general, the *compartmental*  
 879 *direction* of vectorial translocation from the neg-compartment to the pos-compartment is  
 880 defined by assigning the initial and final state as *ergodynamic compartments*,  $H^+_{neg} \rightarrow H^+_{pos}$  or  
 881  $0 = -1 H^+_{neg} + 1 H^+_{pos}$ , related to work (erg = work) that must be performed to lift the proton from  
 882 a lower to a higher electrochemical potential or from the lower to the higher ergodynamic  
 883 compartment (Gnaiger 1993b).

884 In direct analogy to *vectorial* translocation, the direction of a *scalar* chemical reaction,  $A$   
 885  $\rightarrow B$  or  $0 = -1 A + 1 B$ , is defined by assigning substrates and products,  $A$  and  $B$ , as ergodynamic  
 886 compartments. O<sub>2</sub> is defined as a substrate in respiratory O<sub>2</sub> consumption, which together with  
 887 the fuel substrates comprises the substrate compartment of the catabolic reaction (**Fig. 2**).  
 888 Volume-specific scalar O<sub>2</sub> flux is coupled to vectorial translocation, yielding the  $H^+_{pos}/O_2$  ratio  
 889 (**Fig. 1**).

890

### 891 3.2. Normalization for system-size: flux per chamber volume

892

893 **System-specific flux,  $J$ :** The experimental system (the experimental chamber) is part of  
 894 the measurement apparatus, separated from the environment as an isolated, closed, open,  
 895 isothermal or non-isothermal system (**Table 4**). On another level, we distinguish between (1)  
 896 the *system* with volume  $V$  and mass  $m$  defined by the system boundaries, and (2) the *sample* or  
 897 *objects* with volume  $V_X$  and mass  $m_X$  which are enclosed in the experimental chamber (**Fig. 8**).  
 898 Metabolic O<sub>2</sub> flow per object,  $I_{X,O_2}$ , increases as the mass of the object is increased. Object mass-  
 899 specific O<sub>2</sub> flux,  $J_{mX,O_2}$  should be independent of the mass of the object studied in the instrument  
 900 chamber, but system volume-specific O<sub>2</sub> flux,  $J_{V,O_2}$  (per volume of the instrument chamber),  
 901 should increase in direct proportion to the mass of the object in the chamber.  $J_{V,O_2}$  depends on  
 902 mass-concentration of the sample in the chamber, but should be independent of the chamber  
 903 (system) volume. There are practical limitations to increase the mass-concentration of the  
 904 sample in the chamber, when one is concerned about crowding effects and instrumental time  
 905 resolution.

906 When the reactor volume does not change during the reaction, which is typical for liquid  
 907 phase reactions, the volume-specific *flux of a chemical reaction*  $r$  is the time derivative of the  
 908 advancement of the reaction per unit volume,  $J_{V,rB} = d_r \zeta_B / dt \cdot V^{-1}$  [(mol·s<sup>-1</sup>)·L<sup>-1</sup>]. The *rate of*  
 909 *concentration change* is  $dc_B / dt$  [(mol·L<sup>-1</sup>)·s<sup>-1</sup>], where concentration is  $c_B = n_B / V$ . There is a  
 910 difference between (1)  $J_{V,rO_2}$  [mol·s<sup>-1</sup>·L<sup>-1</sup>] and (2) rate of concentration change [mol·L<sup>-1</sup>·s<sup>-1</sup>].  
 911 These merge to a single expression only in closed systems. In open systems, external fluxes  
 912 (such as O<sub>2</sub> supply) are distinguished from internal transformations (metabolic flux, O<sub>2</sub>  
 913 consumption). In a closed system, external flows of all substances are zero and O<sub>2</sub> consumption  
 914 (internal flow of catabolic reactions  $k$ ),  $I_{kO_2}$  [pmol·s<sup>-1</sup>], causes a decline of the amount of O<sub>2</sub> in  
 915 the system,  $n_{O_2}$  [nmol]. Normalization of these quantities for the volume of the system,  $V$  [L  $\equiv$

916  $\text{dm}^3$ ], yields volume-specific  $\text{O}_2$  flux,  $J_{V,\text{kO}_2} = I_{\text{kO}_2}/V$  [ $\text{nmol}\cdot\text{s}^{-1}\cdot\text{L}^{-1}$ ], and  $\text{O}_2$  concentration,  $[\text{O}_2]$   
 917 or  $c_{\text{O}_2} = n_{\text{O}_2}/V$  [ $\mu\text{mol}\cdot\text{L}^{-1} = \mu\text{M} = \text{nmol}\cdot\text{mL}^{-1}$ ]. Instrumental background  $\text{O}_2$  flux is due to external  
 918 flux into a non-ideal closed respirometer; then total volume-specific flux has to be corrected for  
 919 instrumental background  $\text{O}_2$  flux— $\text{O}_2$  diffusion into or out of the instrumental chamber.  $J_{V,\text{kO}_2}$   
 920 is relevant mainly for methodological reasons and should be compared with the accuracy of  
 921 instrumental resolution of background-corrected flux, e.g.,  $\pm 1 \text{ nmol}\cdot\text{s}^{-1}\cdot\text{L}^{-1}$  (Gnaiger 2001).  
 922 ‘Metabolic’ or catabolic indicates  $\text{O}_2$  flux,  $J_{\text{kO}_2}$ , corrected for: (1) instrumental background  $\text{O}_2$   
 923 flux; (2) chemical background  $\text{O}_2$  flux due to autoxidation of chemical components added to  
 924 the incubation medium; and (3) *Rox* for  $\text{O}_2$ -consuming side reactions unrelated to the catabolic  
 925 pathway *k*.

### 927 3.3. Normalization: per sample

928  
 929 The challenges of measuring mitochondrial respiratory flux are matched by those of  
 930 normalization. Application of common and defined units is required for direct transfer of  
 931 reported results into a database. The second [s] is the *SI* unit for the base quantity *time*. It is also  
 932 the standard time-unit used in solution chemical kinetics. A rate may be considered as the  
 933 numerator and normalization as the complementary denominator, which are tightly linked in  
 934 reporting the measurements in a format commensurate with the requirements of a database.  
 935 Normalization (Table 4) is guided by physicochemical principles, methodological  
 936 considerations (Fig. 9), and conceptual strategies (Fig. 10).

937  
 938 **Table 4. Sample concentrations and normalization of flux.**

Expression	Symbol	Definition	Unit	Notes
<b>Sample</b>				
identity of sample	$X$	object: cell, tissue, animal, patient		
number of sample entities $X$	$N_X$	number of objects	x	
mass of sample $X$	$m_X$		kg	1
mass of object $X$	$M_X$	$M_X = m_X \cdot N_X^{-1}$	$\text{kg}\cdot\text{x}^{-1}$	1
<b>Mitochondria</b>				
Mitochondria	mt	$X = \text{mt}$		
amount of mt-elements	$mtE$	quantity of mt-marker	mtEU	
<b>Concentrations</b>				
object number concentration	$C_{NX}$	$C_{NX} = N_X \cdot V^{-1}$	$\text{x}\cdot\text{m}^{-3}$	2
sample mass concentration	$C_{mX}$	$C_{mX} = m_X \cdot V^{-1}$	$\text{kg}\cdot\text{m}^{-3}$	
mitochondrial concentration	$C_{mtE}$	$C_{mtE} = mtE \cdot V^{-1}$	$\text{mtEU}\cdot\text{m}^{-3}$	3
specific mitochondrial density	$D_{mtE}$	$D_{mtE} = mtE \cdot m_X^{-1}$	$\text{mtEU}\cdot\text{kg}^{-1}$	4
mitochondrial content, $mtE$ per object $X$	$mtE_X$	$mtE_X = mtE \cdot N_X^{-1}$	$\text{mtEU}\cdot\text{x}^{-1}$	5
<b><math>\text{O}_2</math> flow and flux</b>				
flow, system	$I_{\text{O}_2}$	internal flow	$\text{mol}\cdot\text{s}^{-1}$	6
volume-specific flux	$J_{V,\text{O}_2}$	$J_{V,\text{O}_2} = I_{\text{O}_2} \cdot V^{-1}$	$\text{mol}\cdot\text{s}^{-1}\cdot\text{m}^{-3}$	7
flow per object $X$	$I_{X,\text{O}_2}$	$I_{X,\text{O}_2} = J_{V,\text{O}_2} \cdot C_{NX}^{-1}$	$\text{mol}\cdot\text{s}^{-1}\cdot\text{x}^{-1}$	8
mass-specific flux	$J_{mX,\text{O}_2}$	$J_{mX,\text{O}_2} = J_{V,\text{O}_2} \cdot C_{mX}^{-1}$	$\text{mol}\cdot\text{s}^{-1}\cdot\text{kg}^{-1}$	9
mitochondria-specific flux	$J_{mtE,\text{O}_2}$	$J_{mtE,\text{O}_2} = J_{V,\text{O}_2} \cdot C_{mtE}^{-1}$	$\text{mol}\cdot\text{s}^{-1}\cdot\text{mtEU}^{-1}$	10

- 940 1 The SI prefix k is used for the SI base unit of mass (kg = 1,000 g). In praxis, various SI prefixes are  
 941 used for convenience, to make numbers easily readable, e.g., 1 mg tissue, cell or mitochondrial mass  
 942 instead of 0.000001 kg.
- 943 2 In case sample  $X = \text{cells}$ , the object number concentration is  $C_{N\text{cell}} = N_{\text{cell}} \cdot V^{-1}$ , and volume may be  
 944 expressed in  $[\text{dm}^3 \equiv \text{L}]$  or  $[\text{cm}^3 = \text{mL}]$ . See **Table 5** for different object types.
- 945 3 mt-concentration is an experimental variable, dependent on sample concentration: (1)  $C_{\text{mtE}} = \text{mtE} \cdot V^{-1}$ ;  
 946 (2)  $C_{\text{mtE}} = \text{mtE}_X \cdot C_{NX}$ ; (3)  $C_{\text{mtE}} = C_{mX} \cdot D_{\text{mtE}}$ .
- 947 4 If the amount of mitochondria,  $\text{mtE}$ , is expressed as mitochondrial mass, then  $D_{\text{mtE}}$  is the mass  
 948 fraction of mitochondria in the sample. If  $\text{mtE}$  is expressed as mitochondrial volume,  $V_{\text{mt}}$ , and the  
 949 mass of sample,  $m_X$ , is replaced by volume of sample,  $V_X$ , then  $D_{\text{mtE}}$  is the volume fraction of  
 950 mitochondria in the sample.
- 951 5  $\text{mtE}_X = \text{mtE} \cdot N_X^{-1} = C_{\text{mtE}} \cdot C_{NX}^{-1}$ .
- 952 6  $\text{O}_2$  can be replaced by other chemicals B to study different reactions, e.g., ATP,  $\text{H}_2\text{O}_2$ , or  
 953 compartmental translocations, e.g.,  $\text{Ca}^{2+}$ .
- 954 7  $I_{\text{O}_2}$  and  $V$  are defined per instrument chamber as a system of constant volume (and constant  
 955 temperature), which may be closed or open.  $I_{\text{O}_2}$  is abbreviated for  $I_{\text{O}_2r}$ —the metabolic or internal  $\text{O}_2$   
 956 flow of the chemical reaction  $r$  in which  $\text{O}_2$  is consumed—hence the negative stoichiometric number,  
 957  $\nu_{\text{O}_2} = -1$ .  $I_{\text{O}_2r} = d_r n_{\text{O}_2} / dt \cdot \nu_{\text{O}_2}^{-1}$ . If  $r$  includes all chemical reactions in which  $\text{O}_2$  participates, then  $d_r n_{\text{O}_2} = dn_{\text{O}_2}$   
 958  $- d_e n_{\text{O}_2}$ , where  $dn_{\text{O}_2}$  is the change in the amount of  $\text{O}_2$  in the instrument chamber and  $d_e n_{\text{O}_2}$  is the  
 959 amount of  $\text{O}_2$  added externally to the system. At steady state, by definition  $dn_{\text{O}_2} = 0$ , hence  $d_r n_{\text{O}_2} = -$   
 960  $d_e n_{\text{O}_2}$ .
- 961 8  $J_{V,\text{O}_2}$  is an experimental variable, expressed per volume of the instrument chamber.
- 962 9  $I_{X,\text{O}_2}$  is a physiological variable, depending on the size of entity  $X$ .
- 963 10 There are many ways to normalize for a mitochondrial marker, that are used in different experimental  
 964 approaches: (1)  $J_{\text{mtE},\text{O}_2} = J_{V,\text{O}_2} \cdot C_{\text{mtE}}^{-1}$ ; (2)  $J_{\text{mtE},\text{O}_2} = J_{V,\text{O}_2} \cdot C_{mX}^{-1} \cdot D_{\text{mtE}}^{-1} = J_{mX,\text{O}_2} \cdot D_{\text{mtE}}^{-1}$ ; (3)  $J_{\text{mtE},\text{O}_2} =$   
 965  $J_{V,\text{O}_2} \cdot C_{NX}^{-1} \cdot \text{mtE}_X^{-1} = I_{X,\text{O}_2} \cdot \text{mtE}_X^{-1}$ ; (4)  $J_{\text{mtE},\text{O}_2} = I_{\text{O}_2} \cdot \text{mtE}^{-1}$ . The mt-elemental unit [mtEU] varies between  
 966 different mt-markers.

**Table 5. Sample types, X, abbreviations, and quantification.**

Identity of sample	$X$	$N_X$	Mass <sup>a</sup>	Volume	mt-Marker
mitochondrial preparation	mtprep	[x]	[kg]	[m <sup>3</sup> ]	[mtEU]
isolated mitochondria	imt		$m_{\text{mt}}$	$V_{\text{mt}}$	$\text{mtE}$
tissue homogenate	thom		$m_{\text{thom}}$		$\text{mtE}_{\text{thom}}$
permeabilized tissue	pti		$m_{\text{pti}}$		$\text{mtE}_{\text{pti}}$
permeabilized fibre	pfi		$m_{\text{pfi}}$		$\text{mtE}_{\text{pfi}}$
permeabilized cell	pce	$N_{\text{pce}}$	$M_{\text{pce}}$	$V_{\text{pce}}$	$\text{mtE}_{\text{pce}}$
intact cell	ce	$N_{\text{ce}}$	$M_{\text{ce}}$	$V_{\text{ce}}$	$\text{mtE}_{\text{ce}}$
Organism	org	$N_{\text{org}}$	$M_{\text{org}}$	$V_{\text{org}}$	

969 <sup>a</sup> Instead of mass, frequently the wet weight or dry weight is stated,  $W_w$  or  $W_d$ .  
 970  $m_X$  is mass of the sample [kg],  $M_X$  is mass of the object  $[\text{kg} \cdot \text{x}^{-1}]$ .

971  
 972 **Sample concentration,  $C_{mX}$ :** Normalization for sample concentration is required to  
 973 report respiratory data. Considering a tissue or cells as the sample,  $X$ , the sample mass is  $m_X$   
 974 [mg] from which a mitochondrial preparation is obtained.  $m_X$  is frequently measured as wet or  
 975 dry weight,  $W_w$  or  $W_d$  [mg], or as amount of tissue or cell protein,  $m_{\text{Protein}}$ . In the case of  
 976 permeabilized tissues, cells, and homogenates, the sample concentration,  $C_{mX} = m_X / V$   $[\text{mg} \cdot \text{mL}^{-1}$   
 977  $= \text{g} \cdot \text{L}^{-1}]$ , is simply the mass of the subsample of tissue that is transferred into the instrument  
 978 chamber.

979 **Mass-specific flux,  $J_{mX,\text{O}_2}$ :** Mass-specific flux is obtained by expressing respiration per  
 980 mass of sample,  $m_X$  [mg].  $X$  is the type of sample—tissue homogenate, permeabilized fibres or  
 981 cells. Volume-specific flux is divided by mass concentration of  $X$ ,  $J_{mX,\text{O}_2} = J_{V,\text{O}_2} / C_{mX}$ ; or flow  
 982 per cell is divided by mass per cell,  $J_{m\text{cell},\text{O}_2} = I_{\text{cell},\text{O}_2} / M_{\text{cell}}$ . If mass-specific  $\text{O}_2$  flux is constant  
 983 and independent of sample size (expressed as mass), then there is no interaction between the  
 984 subsystems. A 1.5 mg and a 3.0 mg muscle sample respire at identical mass-specific flux.  
 985 Mass-specific  $\text{O}_2$  flux, however, may change with the mass of a tissue sample, cells or isolated

986 mitochondria in the measuring chamber, in which the nature of the interaction becomes an issue.  
 987 Therefore, cell density must be optimization, particularly in experiments carried out in wells,  
 988 considering the confluency of the cell monolayer or clumps of cells (Salabei *et al.* 2014).

989 **Number concentration,  $C_{NX}$ :**  $C_{NX}$  is the experimental *number concentration* of sample  
 990  $X$ . In the case of cells or animals, *e.g.*, nematodes,  $C_{NX} = N_X/V [X \cdot L^{-1}]$ , where  $N_X$  is the number  
 991 of cells or organisms in the chamber (**Table 4**).

992 **Flow per object,  $I_{X,O_2}$ :** A special case of normalization is encountered in respiratory  
 993 studies with permeabilized (or intact) cells. If respiration is expressed per cell, the  $O_2$  flow per  
 994 measurement system is replaced by the  $O_2$  flow per cell,  $I_{cell,O_2}$  (**Table 4**).  $O_2$  flow can be  
 995 calculated from volume-specific  $O_2$  flux,  $J_{V,O_2} [nmol \cdot s^{-1} \cdot L^{-1}]$  (per  $V$  of the measurement chamber  
 996 [L]), divided by the number concentration of cells,  $C_{N_{ce}} = N_{ce}/V [cell \cdot L^{-1}]$ , where  $N_{ce}$  is the  
 997 number of cells in the chamber. Cellular  $O_2$  flow can be compared between cells of identical  
 998 size. To take into account changes and differences in cell size, normalization is required to  
 999 obtain cell size-specific or mitochondrial marker-specific  $O_2$  flux (Renner *et al.* 2003).

1000 The complexity changes when the sample is a whole organism studied as an experimental  
 1001 model. The scaling law in respiratory physiology reveals a strong interaction of  $O_2$  consumption  
 1002 and individual body mass of an organism, since *basal* metabolic rate (flow) does not increase  
 1003 linearly with body mass, whereas *maximum* mass-specific  $O_2$  flux,  $\dot{V}_{O_2max}$  or  $\dot{V}_{O_2peak}$ , is  
 1004 approximately constant across a large range of individual body mass (Weibel and Hoppeler  
 1005 2005), with individuals, breeds, and species deviating substantially from this relationship.  
 1006  $\dot{V}_{O_2peak}$  of human endurance athletes is 60 to 80 mL  $O_2 \cdot min^{-1} \cdot kg^{-1}$  body mass, converted to  
 1007  $J_{M,O_2peak}$  of 45 to 60  $nmol \cdot s^{-1} \cdot g^{-1}$  (Gnaiger 2014; **Table 6**).

1008

### 1009 3.4. Normalization for mitochondrial content

1010

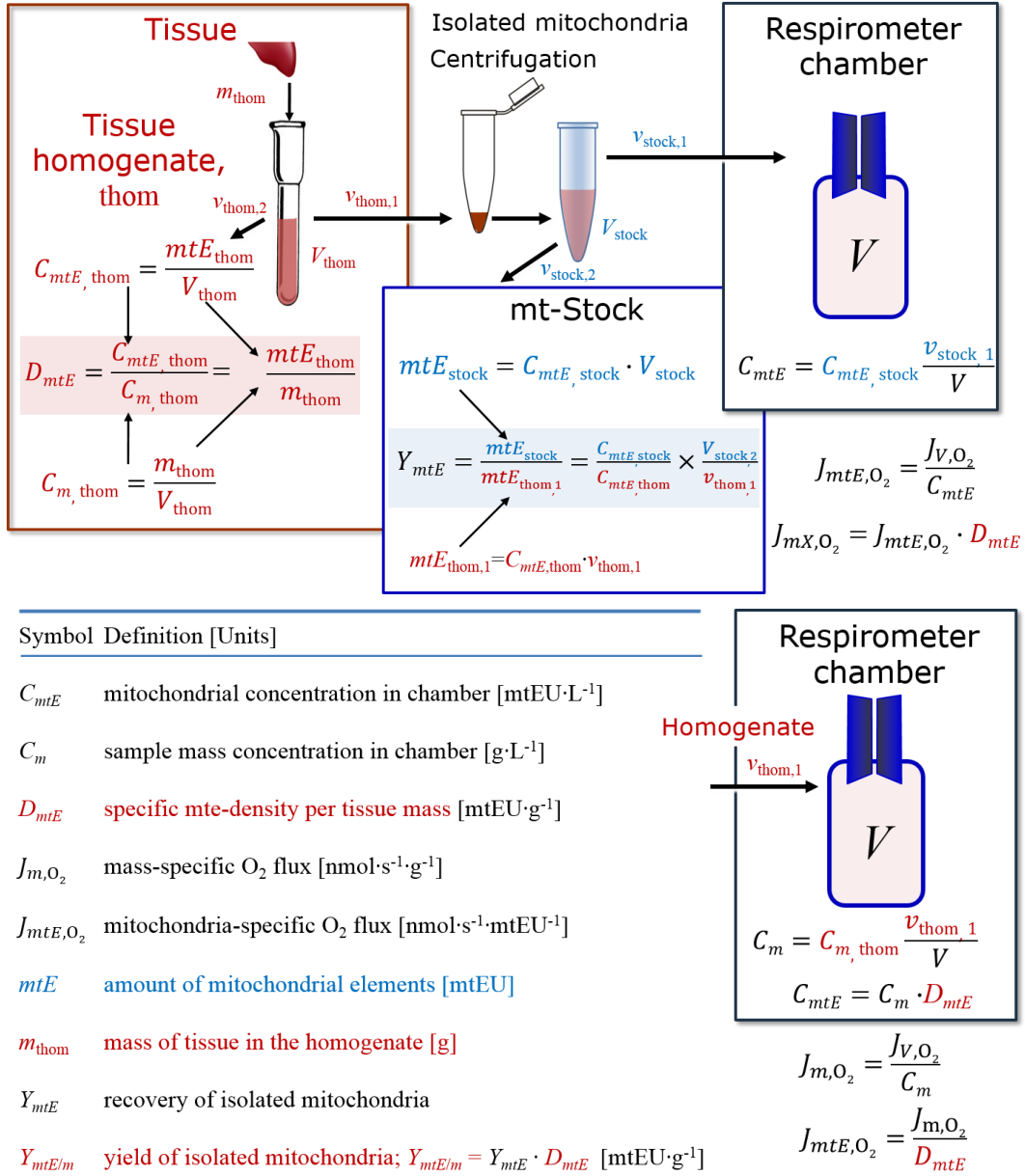
1011 Tissues can contain multiple cell populations that may have distinct mitochondrial  
 1012 subtypes. Mitochondria undergo dynamic fission and fusion cycles, and can exist in multiple  
 1013 stages and sizes which may be altered by a range of factors. The isolation of mitochondria (often  
 1014 achieved through differential centrifugation) can therefore yield a subsample of the  
 1015 mitochondrial types present in a tissue, depending on isolation protocols utilized (*e.g.*,  
 1016 centrifugation speed). This possible bias should be taken into account when planning  
 1017 experiments using isolated mitochondria. Different sizes of mitochondria are enriched at  
 1018 specific centrifugation speeds, which is used for isolation of mitochondrial subpopulations.

1019 Part of the mitochondrial content of a tissue is lost during preparation of isolated  
 1020 mitochondria. The fraction of mitochondria in the isolate is expressed as mitochondrial  
 1021 recovery (**Fig. 9**). At a high mitochondrial recovery the sample of isolated mitochondria is more  
 1022 representative of the total mitochondrial population than in preparations characterized by low  
 1023 recovery. Determination of the mitochondrial recovery and yield is based on measurement of  
 1024 the concentration of a mitochondrial marker in the tissue homogenate,  $C_{mtE,thom}$ , which  
 1025 simultaneously provides information on the specific mitochondrial density in the sample (**Fig.**  
 1026 **9**).

1027 Normalization is a problematic subject; it is essential to consider the question of the study.  
 1028 If the study aims at comparing tissue performance—such as the effects of a treatment on a  
 1029 specific tissue, then normalization can be successful, using tissue mass or protein content, for  
 1030 example. However, if the aim is to find differences on mitochondrial function independent of  
 1031 mitochondrial density (**Table 4**), then normalization to a mitochondrial marker is imperative  
 1032 (**Fig. 10**). One cannot assume that quantitative changes in various markers—such as  
 1033 mitochondrial proteins—necessarily occur in parallel with one another. It should be established  
 1034 that the marker chosen is not selectively altered by the performed treatment. In conclusion, the  
 1035 normalization must reflect the question under investigation to reach a satisfying answer. On the



1036 other hand, the goal of comparing results across projects and institutions requires  
 1037 standardization on normalization for entry into a databank.  
 1038



1040

1041

1042

1043

1044

1045

1046

1047

1048

1049

1050

1051

1052

1053

1054

1055

1056

**Fig. 9. Normalization of volume-specific flux of isolated mitochondria and tissue homogenate.** **A:** Recovery,  $Y_{mtE}$ , in preparation of isolated mitochondria.  $v_{thom,1}$  and  $v_{stock,1}$  are the volumes transferred from the total volume,  $V_{thom}$  and  $V_{stock}$ , respectively.  $mtE_{thom,1}$  is the amount of mitochondrial elements in volume  $v_{thom,1}$  used for isolation. **B:** Homogenate,  $v_{thom,1}$  is transferred directly into the respirometer chamber. See **Table 4** for further symbols.

**Mitochondrial concentration,  $C_{mtE}$ , and mitochondrial markers:** Mitochondrial concentration in the tissue and the measurement chamber are quantified as (1) a physiological output that is the result of mitochondrial biogenesis and degradation, and (2) a quantity for normalization in functional analyses. Mitochondrial organelles comprise a dynamic cellular reticulum in various states of fusion and fission. Hence, the definition of an "amount" of mitochondria is often misconceived: mitochondria cannot be counted reliably as a number of occurring elements. Therefore, quantification of the "amount" of mitochondria depends on the measurement of chosen mitochondrial markers. 'Mitochondria are the structural and functional elemental units of cell respiration' (Gnaiger 2014). The quantity of a mitochondrial marker can

1057 reflect the amount of *mitochondrial elements*, *mtE*, expressed in various mitochondrial  
 1058 elemental units [mtEU] specific for each measured mt-marker (**Table 4**). However, since  
 1059 mitochondrial quality may change in response to stimuli—particularly in mitochondrial  
 1060 dysfunction and after exercise training (Pesta *et al.* 2011; Campos *et al.* 2017)—some markers  
 1061 can vary while others are unchanged: (1) Mitochondrial volume and membrane area are  
 1062 structural markers, whereas mitochondrial protein mass is frequently used as a marker for  
 1063 isolated mitochondria. (2) Molecular and enzymatic mitochondrial markers (amounts or  
 1064 activities) can be selected as matrix markers, *e.g.*, citrate synthase activity, mtDNA; mtIM-  
 1065 markers, *e.g.*, cytochrome *c* oxidase activity, *aa*<sub>3</sub> content, cardiolipin, or mtOM-markers, *e.g.*,  
 1066 TOM20. (3) Extending the measurement of mitochondrial marker enzyme activity to  
 1067 mitochondrial pathway capacity, ET- or OXPHOS-capacity can be considered as an integrative  
 1068 functional mitochondrial marker.  
 1069

<b>Flow, Performance</b>	=	<b>Element function</b>	x	<b>Element density</b>	x	<b>Size of entity</b>
$\frac{\text{mol}\cdot\text{s}^{-1}}{x}$	=	$\frac{\text{mol}\cdot\text{s}^{-1}}{x_{\text{mte}}}$	·	$\frac{x_{\text{mte}}}{\text{kg}}$	·	$\frac{\text{kg}}{x}$

<b>A</b>	<b>Flow</b>	=	<b>mt-specific flux</b>	x	<b>mt-structure, functional elements</b>
	$I_{X,O_2}$	=	$J_{\text{mte},O_2}$	·	$\text{mte}_X$
					$\frac{\text{mte}_X}{M_X} \cdot M_X$

	$I_{X,O_2}$	=	$J_{\text{mte},O_2}$	·	$D_{\text{mte}}$	·	$M_X$
	$\frac{I_{X,O_2}}{M_X}$	=	$\frac{I_{X,O_2}}{\text{mte}_X}$	·	$\frac{\text{mte}_X}{M_X}$		

<b>B</b>	<b>Flow</b>	=	<b>Entity mass- specific flux</b>	x	<b>Mass of entity</b>
	$I_{X,O_2}$	=	$J_{mX,O_2}$	·	$M_X$

1070  
 1071 **Fig. 10. Structure-function analysis of performance of an organism, organ or tissue, or a**  
 1072 **cell (sample entity, X). O<sub>2</sub> flow,  $I_{X,O_2}$ , is the product of performance per functional element**  
 1073 **(element function, mitochondria-specific flux), element density (mitochondrial density,**  
 1074  **$D_{\text{mtE}}$ ), and size of entity X (mass,  $M_X$ ). (A) Structured analysis: performance is the product of**  
 1075 **mitochondrial function (mt-specific flux) and structure (functional elements;  $D_{\text{mtE}}$  times mass**  
 1076 **of X). (B) Unstructured analysis: performance is the product of entity mass-specific flux,  $J_{mX,O_2}$**   
 1077  **$= I_{X,O_2}/M_X = I_{O_2}/m_X$  [mol·s<sup>-1</sup>·kg<sup>-1</sup>] and size of entity, expressed as mass of X;  $M_X = m_X \cdot N_X^{-1}$**   
 1078 **[kg·x<sup>-1</sup>]. See Table 4 for further explanation of quantities and units. Modified from Gnaiger**  
 1079 **(2014).**

1080  
 1081 Depending on the type of mitochondrial marker, the mitochondrial elements, *mtE*, are  
 1082 expressed in marker-specific units. It is recommended to distinguish *experimental*  
 1083 *mitochondrial concentration*,  $C_{\text{mtE}} = \text{mtE}/V$  and *physiological mitochondrial density*,  $D_{\text{mtE}} =$   
 1084  $\text{mtE}/m_X$ . Then mitochondrial density is the amount of mitochondrial elements per mass of tissue,  
 1085 which is a biological variable (**Fig. 10**). The experimental variable is mitochondrial density  
 1086 multiplied by sample mass concentration in the measuring chamber,  $C_{\text{mtE}} = D_{\text{mtE}} \cdot C_{mX}$ , or  
 1087 mitochondrial content multiplied by sample number concentration,  $C_{\text{mtE}} = \text{mtE}_X \cdot C_{NX}$  (**Table 4**).

1088 **Mitochondria-specific flux,  $J_{\text{mtE},O_2}$ :** Volume-specific metabolic O<sub>2</sub> flux depends on: (1)  
 1089 the sample concentration in the volume of the instrument chamber,  $C_{mX}$ , or  $C_{NX}$ ; (2) the

1090 mitochondrial density in the sample,  $D_{mtE} = mtE/m_X$  or  $mtE_X = mtE/N_X$ ; and (3) the specific  
 1091 mitochondrial activity or performance per elemental mitochondrial unit,  $J_{mtE,O_2} = J_{V,O_2}/C_{mtE}$   
 1092 [ $\text{mol}\cdot\text{s}^{-1}\cdot\text{mtEU}^{-1}$ ] (Table 4). Obviously, the numerical results for  $J_{mtE,O_2}$  vary with the type of  
 1093 mitochondrial marker chosen for measurement of  $mtE$  and  $C_{mtE} = mtE/V$  [ $\text{mtEU}\cdot\text{m}^{-3}$ ].  
 1094

### 1095 3.5. Evaluation of mitochondrial markers

1096  
 1097 Different methods are implicated in the quantification of mitochondrial markers and have  
 1098 different strengths. Some problems are common for all mitochondrial markers,  $mtE$ : (1)  
 1099 Accuracy of measurement is crucial, since even a highly accurate and reproducible  
 1100 measurement of  $O_2$  flux results in an inaccurate and noisy expression normalized for a biased  
 1101 and noisy measurement of a mitochondrial marker. This problem is acute in mitochondrial  
 1102 respiration because the denominators used (the mitochondrial markers) are often small moieties  
 1103 of which accurate and precise determination is difficult. This problem can be avoided when  $O_2$   
 1104 fluxes measured in substrate-uncoupler-inhibitor titration protocols are normalized for flux in  
 1105 a defined respiratory reference state, which is used as an *internal* marker and yields flux control  
 1106 ratios,  $FCRs$  (Fig. 8).  $FCRs$  are independent of any *externally* measured markers and, therefore,  
 1107 are statistically robust, considering the limitations of ratios in general (Jasienski and Bazzaz  
 1108 1999).  $FCRs$  indicate qualitative changes of mitochondrial respiratory control, with highest  
 1109 quantitative resolution, separating the effect of mitochondrial density or concentration on  $J_{mX,O_2}$   
 1110 and  $I_{X,O_2}$  from that of function per elemental mitochondrial marker,  $J_{mtE,O_2}$  (Pesta *et al.* 2011;  
 1111 Gnaiger 2014). (2) If mitochondrial quality does not change and only the amount of  
 1112 mitochondria varies as a determinant of mass-specific flux, any marker is equally qualified in  
 1113 principle; then in practice selection of the optimum marker depends only on the accuracy and  
 1114 precision of measurement of the mitochondrial marker. (3) If mitochondrial flux control ratios  
 1115 change, then there may not be any best mitochondrial marker. In general, measurement of  
 1116 multiple mitochondrial markers enables a comparison and evaluation of normalization for a  
 1117 variety of mitochondrial markers. Particularly during postnatal development, the activity of  
 1118 marker enzymes—such as cytochrome *c* oxidase and citrate synthase—follows different time  
 1119 courses (Drahota *et al.* 2004). Evaluation of mitochondrial markers in healthy controls is  
 1120 insufficient for providing guidelines for application in the diagnosis of pathological states and  
 1121 specific treatments.

1122 In line with the concept of the respiratory control ratio (Chance and Williams 1955a), the  
 1123 most readily used normalization is that of flux control ratios and flux control factors (Gnaiger  
 1124 2014). Selection of the state of maximum flux in a protocol as the reference state has the  
 1125 advantages of: (1) internal normalization; (2) statistical linearization of the response in the range  
 1126 of 0 to 1; and (3) consideration of maximum flux for integrating a large number of elemental  
 1127 steps in the OXPHOS- or ET-pathways. This reduces the risk of selecting a functional marker  
 1128 that is specifically altered by the treatment or pathology, yet increases the chance that the highly  
 1129 integrative pathway is disproportionately affected, *e.g.*, the OXPHOS- rather than ET-pathway  
 1130 in case of an enzymatic defect in the phosphorylation-pathway. In this case, additional  
 1131 information can be obtained by reporting flux control ratios based on a reference state which  
 1132 indicates stable tissue-mass specific flux. Stereological determination of mitochondrial content  
 1133 via two-dimensional transmission electron microscopy can have limitations due to the dynamics  
 1134 of mitochondrial size (Meinild Lundby *et al.* 2017). Accurate determination of three-  
 1135 dimensional volume by two-dimensional microscopy can be both time consuming and  
 1136 statistically challenging (Larsen *et al.* 2012).

1137 The validity of using mitochondrial marker enzymes (citrate synthase activity, Complex  
 1138 I–IV amount or activity) for normalization of flux is limited in part by the same factors that  
 1139 apply to flux control ratios. Strong correlations between various mitochondrial markers and  
 1140 citrate synthase activity (Reichmann *et al.* 1985; Boushel *et al.* 2007; Mogensen *et al.* 2007)

1141 are expected in a specific tissue of healthy subjects and in disease states not specifically  
 1142 targeting citrate synthase. Citrate synthase activity is acutely modifiable by exercise  
 1143 (Tonkonogi *et al.* 1997; Leek *et al.* 2001). Evaluation of mitochondrial markers related to a  
 1144 selected age and sex cohort cannot be extrapolated to provide recommendations for  
 1145 normalization in respirometric diagnosis of disease, in different states of development and  
 1146 ageing, different cell types, tissues, and species. mtDNA normalized to nDNA via qPCR is  
 1147 correlated to functional mitochondrial markers including OXPHOS- and ET-capacity in some  
 1148 cases (Puntschart *et al.* 1995; Wang *et al.* 1999; Menshikova *et al.* 2006; Boushel *et al.* 2007),  
 1149 but lack of such correlations have been reported (Menshikova *et al.* 2005; Schultz and Wiesner  
 1150 2000; Pesta *et al.* 2011). Several studies indicate a strong correlation between cardiolipin  
 1151 content and increase in mitochondrial function with exercise (Menshikova *et al.* 2005;  
 1152 Menshikova *et al.* 2007; Larsen *et al.* 2012; Faber *et al.* 2014), but its use as a general  
 1153 mitochondrial biomarker in disease remains questionable.

1154

### 1155 3.6. Conversion: units

1156

1157 Many different units have been used to report the rate of oxygen consumption, OCR  
 1158 (**Table 6**). *SI* base units provide the common reference to introduce the theoretical principles  
 1159 (**Fig. 8**), and are used with appropriately chosen *SI* prefixes to express numerical data in the  
 1160 most practical format, with an effort towards unification within specific areas of application  
 1161 (**Table 7**). Reporting data in *SI* units—including the mole [mol], coulomb [C], joule [J], and  
 1162 second [s]—should be encouraged, particularly by journals which propose the use of *SI* units.

1163 Although volume is expressed as  $\text{m}^3$  using the *SI* base unit, the litre [ $\text{dm}^3$ ] is a  
 1164 conventional unit of volume for concentration and is used for most solution chemical kinetics.  
 1165 If one multiplies  $I_{\text{cell},\text{O}_2}$  by  $C_{N_{\text{cell}}}$ , then the result will not only be the amount of  $\text{O}_2$  [mol]  
 1166 consumed per time [ $\text{s}^{-1}$ ] in one litre [ $\text{L}^{-1}$ ], but also the change in the concentration of oxygen per  
 1167 second (for any volume of an ideally closed system). This is ideal for kinetic modeling as it  
 1168 blends with chemical rate equations where concentrations are typically expressed in  $\text{mol}\cdot\text{L}^{-1}$   
 1169 (Wagner *et al.* 2011). In studies of multinuclear cells—such as differentiated skeletal muscle  
 1170 cells—it is easy to determine the number of nuclei but not the total number of cells. A  
 1171 generalized concept, therefore, is obtained by substituting cells by nuclei as the sample entity.  
 1172 This does not hold, however, for enucleated platelets.

1173 For studies of cells, we recommend that respiration be expressed, as far as possible, as:  
 1174 (1)  $\text{O}_2$  flux normalized for a mitochondrial marker, for separation of the effects of mitochondrial  
 1175 quality and content on cell respiration (this includes *FCRs* as a normalization for a functional  
 1176 mitochondrial marker); (2)  $\text{O}_2$  flux in units of cell volume or mass, for comparison of respiration  
 1177 of cells with different cell size (Renner *et al.* 2003) and with studies on tissue preparations, and  
 1178 (3)  $\text{O}_2$  flow in units of attomole ( $10^{-18}$  mol) of  $\text{O}_2$  consumed in a second by each cell  
 1179 [ $\text{amol}\cdot\text{s}^{-1}\cdot\text{cell}^{-1}$ ], numerically equivalent to [ $\text{pmol}\cdot\text{s}^{-1}\cdot 10^{-6}$  cells]. This convention allows  
 1180 information to be easily used when designing experiments in which oxygen consumption must  
 1181 be considered. For example, to estimate the volume-specific  $\text{O}_2$  flux in an instrument chamber  
 1182 that would be expected at a particular cell number concentration, one simply needs to multiply  
 1183 the flow per cell by the number of cells per volume of interest. This provides the amount of  $\text{O}_2$   
 1184 [mol] consumed per time [ $\text{s}^{-1}$ ] per unit volume [ $\text{L}^{-1}$ ]. At an  $\text{O}_2$  flow of  $100 \text{ amol}\cdot\text{s}^{-1}\cdot\text{cell}^{-1}$  and a  
 1185 cell density of  $10^9 \text{ cells}\cdot\text{L}^{-1}$  ( $10^6 \text{ cells}\cdot\text{mL}^{-1}$ ), the volume-specific  $\text{O}_2$  flux is  $100 \text{ nmol}\cdot\text{s}^{-1}\cdot\text{L}^{-1}$  ( $100$   
 1186  $\text{pmol}\cdot\text{s}^{-1}\cdot\text{mL}^{-1}$ ).

1187

1188

1189

1190

1191  
1192  
1193  
1194**Table 6. Conversion of various units used in respirometry and ergometry.**  $e^-$  is the number of electrons or reducing equivalents.  $z_B$  is the charge number of entity B.

1 Unit	x	Multiplication factor	SI-unit	Note
ng.atom O $\cdot$ s $^{-1}$	(2 e $^-$ )	0.5	nmol O $_2$ $\cdot$ s $^{-1}$	
ng.atom O $\cdot$ min $^{-1}$	(2 e $^-$ )	8.33	pmol O $_2$ $\cdot$ s $^{-1}$	
natom O $\cdot$ min $^{-1}$	(2 e $^-$ )	8.33	pmol O $_2$ $\cdot$ s $^{-1}$	
nmol O $_2$ $\cdot$ min $^{-1}$	(4 e $^-$ )	16.67	pmol O $_2$ $\cdot$ s $^{-1}$	
nmol O $_2$ $\cdot$ h $^{-1}$	(4 e $^-$ )	0.2778	pmol O $_2$ $\cdot$ s $^{-1}$	
mL O $_2$ $\cdot$ min $^{-1}$ at STPD <sup>a</sup>		0.744	$\mu$ mol O $_2$ $\cdot$ s $^{-1}$	1
W = J/s at -470 kJ/mol O $_2$		-2.128	$\mu$ mol O $_2$ $\cdot$ s $^{-1}$	
mA = mC $\cdot$ s $^{-1}$	( $z_{H^+} = 1$ )	10.36	nmol H $^+$ $\cdot$ s $^{-1}$	2
mA = mC $\cdot$ s $^{-1}$	( $z_{O_2} = 4$ )	2.59	nmol O $_2$ $\cdot$ s $^{-1}$	2
nmol H $^+$ $\cdot$ s $^{-1}$	( $z_{H^+} = 1$ )	0.09649	mA	3
nmol O $_2$ $\cdot$ s $^{-1}$	( $z_{O_2} = 4$ )	0.38594	mA	3

1195  
1196  
1197  
1198  
1199  
1200  
1201  
1202  
1203  
1204

- 1 At standard temperature and pressure dry (STPD: 0 °C = 273.15 K and 1 atm = 101.325 kPa = 760 mmHg), the molar volume of an ideal gas,  $V_m$ , and  $V_{m,O_2}$  is 22.414 and 22.392 L $\cdot$ mol $^{-1}$ , respectively. Rounded to three decimal places, both values yield the conversion factor of 0.744. For comparison at NTPD (20 °C),  $V_{m,O_2}$  is 24.038 L $\cdot$ mol $^{-1}$ . Note that the SI standard pressure is 100 kPa.
- 2 The multiplication factor is  $10^6/(z_B \cdot F)$ .
- 3 The multiplication factor is  $z_B \cdot F/10^6$ .

**Table 7. Conversion of units with preservation of numerical values.**

Name	Frequently used unit	Equivalent unit	Note
volume-specific flux, $J_{V,O_2}$	pmol $\cdot$ s $^{-1}$ $\cdot$ mL $^{-1}$	nmol $\cdot$ s $^{-1}$ $\cdot$ L $^{-1}$	1
	nmol $\cdot$ s $^{-1}$ $\cdot$ L $^{-1}$	mol $\cdot$ s $^{-1}$ $\cdot$ m $^{-3}$	
cell-specific flow, $I_{O_2}$	pmol $\cdot$ s $^{-1}$ $\cdot$ 10 $^{-6}$ cells	amol $\cdot$ s $^{-1}$ $\cdot$ cell $^{-1}$	2
	pmol $\cdot$ s $^{-1}$ $\cdot$ 10 $^{-9}$ cells	zmol $\cdot$ s $^{-1}$ $\cdot$ cell $^{-1}$	3
cell number concentration, $C_{Nce}$	10 $^6$ cells $\cdot$ mL $^{-1}$	10 $^9$ cells $\cdot$ L $^{-1}$	
mitochondrial protein concentration, $C_{mtE}$	0.1 mg $\cdot$ mL $^{-1}$	0.1 g $\cdot$ L $^{-1}$	
mass-specific flux, $J_{m,O_2}$	pmol $\cdot$ s $^{-1}$ $\cdot$ mg $^{-1}$	nmol $\cdot$ s $^{-1}$ $\cdot$ g $^{-1}$	4
catabolic power, $P_k$	$\mu$ W $\cdot$ 10 $^{-6}$ cells	pW $\cdot$ cell $^{-1}$	1
Volume	1,000 L	m $^3$ (1,000 kg)	
	L	dm $^3$ (kg)	
	mL	cm $^3$ (g)	
	$\mu$ L	mm $^3$ (mg)	
	fL	$\mu$ m $^3$ (pg)	5
amount of substance concentration	M = mol $\cdot$ L $^{-1}$	mol $\cdot$ dm $^{-3}$	

1205  
1206  
1207  
1208  
1209

- 1 pmol: picomole = 10 $^{-12}$  mol
- 2 amol: attomole = 10 $^{-18}$  mol
- 3 zmol: zeptomole = 10 $^{-21}$  mol
- 4 nmol: nanomole = 10 $^{-9}$  mol
- 5 fL: femtolitre = 10 $^{-15}$  L

1210 ET-capacity in human cell types including HEK 293, primary HUVEC and fibroblasts  
 1211 ranges from 50 to 180  $\text{amol}\cdot\text{s}^{-1}\cdot\text{cell}^{-1}$ , measured in intact cells in the noncoupled state (see  
 1212 Gnaiger 2014). At 100  $\text{amol}\cdot\text{s}^{-1}\cdot\text{cell}^{-1}$  corrected for *Rox*, the current across the mt-membranes,  
 1213  $I_{\text{eH}^+}$ , approximates 193  $\text{pA}\cdot\text{cell}^{-1}$  or 0.2 nA per cell. See Rich (2003) for an extension of  
 1214 quantitative bioenergetics from the molecular to the human scale, with a transmembrane proton  
 1215 flux equivalent to 520 A in an adult at a catabolic power of -110 W. Modelling approaches  
 1216 illustrate the link between protonmotive force and currents (Willis *et al.* 2016).

1217 We consider isolated mitochondria as powerhouses and proton pumps as molecular  
 1218 machines to relate experimental results to energy metabolism of the intact cell. The cellular  
 1219  $\text{P}\gg/\text{O}_2$  based on oxidation of glycogen is increased by the glycolytic (fermentative) substrate-  
 1220 level phosphorylation of 3  $\text{P}\gg/\text{Glyc}$  or 0.5 mol  $\text{P}\gg$  for each mol  $\text{O}_2$  consumed in the complete  
 1221 oxidation of a mol glycosyl unit (Glyc). Adding 0.5 to the mitochondrial  $\text{P}\gg/\text{O}_2$  ratio of 5.4  
 1222 yields a bioenergetic cell physiological  $\text{P}\gg/\text{O}_2$  ratio close to 6. Two NADH equivalents are  
 1223 formed during glycolysis and transported from the cytosol into the mitochondrial matrix, either  
 1224 by the malate-aspartate shuttle or by the glycerophosphate shuttle resulting in different  
 1225 theoretical yields of ATP generated by mitochondria, the energetic cost of which potentially  
 1226 must be taken into account. Considering also substrate-level phosphorylation in the TCA cycle,  
 1227 this high  $\text{P}\gg/\text{O}_2$  ratio not only reflects proton translocation and OXPHOS studied in isolation,  
 1228 but integrates mitochondrial physiology with energy transformation in the living cell (Gnaiger  
 1229 1993a).

1230

1231

#### 1232 4. Conclusions

1233

1234 MitoEAGLE can serve as a gateway to better diagnose mitochondrial respiratory defects  
 1235 linked to genetic variation, age-related health risks, sex-specific mitochondrial performance,  
 1236 lifestyle with its effects on degenerative diseases, and thermal and chemical environment. The  
 1237 present recommendations on coupling control states and rates, linked to the concept of the  
 1238 protonmotive force, are focused on studies with mitochondrial preparations. These will be  
 1239 extended in a series of reports on pathway control of mitochondrial respiration, respiratory  
 1240 states in intact cells, and harmonization of experimental procedures.

1241 The optimal choice for expressing mitochondrial and cell respiration (**Box 3**) as  $\text{O}_2$  flow  
 1242 per biological system, and normalization for specific tissue-markers (volume, mass, protein)  
 1243 and mitochondrial markers (volume, protein, content, mtDNA, activity of marker enzymes,  
 1244 respiratory reference state) is guided by the scientific question under study. Interpretation of  
 1245 the obtained data depends critically on appropriate normalization, and therefore reporting rates  
 1246 merely as  $\text{nmol}\cdot\text{s}^{-1}$  is discouraged, since it restricts the analysis to intra-experimental  
 1247 comparison of relative (qualitative) differences. Expressing  $\text{O}_2$  consumption per cell may not  
 1248 be possible when dealing with tissues. For studies with mitochondrial preparations, we  
 1249 recommend that normalizations be provided as far as possible: (1) on a per cell basis as  $\text{O}_2$  flow  
 1250 (a biophysical normalization); (2) per g cell or tissue protein, or per cell or tissue mass as mass-  
 1251 specific  $\text{O}_2$  flux (a cellular normalization); and (3) per mitochondrial marker as mt-specific flux  
 1252 (a mitochondrial normalization). With information on cell size and the use of multiple  
 1253 normalizations, maximum potential information is available (Renner *et al.* 2003; Wagner *et al.*  
 1254 2011; Gnaiger 2014).

1255 When using isolated mitochondria, total mitochondrial protein is a frequently applied  
 1256 mitochondrial marker, the use of which is restricted to isolated mitochondria. The  
 1257 mitochondrial recovery and yield, and experimental criteria for evaluation of purity versus  
 1258 integrity should be reported. Mitochondrial markers—such as citrate synthase activity as an  
 1259 enzymatic matrix marker—provide a link to the tissue of origin on the basis of calculating the

1260 mitochondrial recovery, *i.e.*, the fraction of mitochondrial marker obtained from a unit mass of  
 1261 tissue.

1262

1263 **Table 8. Terms, symbols, and units.**

Term	Symbol	SI unit	Links and comments
1269 alternative quinol oxidase	AOX		Fig. 1
1270 amount of substance B	$n_B$	[mol]	
1271 apparent equilibrium constant	$K_m'$		
1272 Complexes I to IV	CI to CIV		respiratory ET Complexes; Fig. 1
1273 concentration of substance B	$c_B = n_B \cdot V^{-1}$ ; [B]	[mol·m <sup>-3</sup> ]	Box 2
1274 electron transfer system	ETS		
1275 flow, for substance B	$I_B$	[mol·s <sup>-1</sup> ]	system-related extensive quantity; Fig. 8
1276 flux, for substance B	$J_B$	<i>varies</i>	size-specific quantity; Fig. 8
1277 inorganic phosphate	$P_i$		
1278 LEAK	LEAK		Tab. 1
1279 mass of sample X	$m_X$	[kg]	Tab. 4
1280 mass of entity X	$M_X$	[kg]	Tab. 4
1281 MITOCARTA			<a href="https://www.broadinstitute.org/scientific-community/science/programs/metabolic-disease-program/publications/mitocarta/mitocarta-in-0">https://www.broadinstitute.org/scientific-community/science/programs/metabolic-disease-program/publications/mitocarta/mitocarta-in-0</a>
1282			
1283			
1284			
1285			
1286 MitoPedia			<a href="http://www.bioblast.at/index.php/MitoPedia">http://www.bioblast.at/index.php/MitoPedia</a>
1287 mitochondria or mitochondrial	mt		Box 1
1288 mitochondrial DNA	mtDNA		Box 1
1289 mitochondrial concentration	$C_{mtE} = mtE \cdot V^{-1}$	[mtEU·m <sup>-3</sup> ]	Tab. 4
1290 mitochondrial content	$mtE_X = mtE \cdot N_X^{-1}$	[mtEU·x <sup>-1</sup> ]	Tab. 4
1291 mitochondrial elemental unit	mtEU	<i>varies</i>	Tab. 4, specific units for mt-marker
1292 mitochondrial inner membrane	mtIM		MIM is widely used, and M is replaced by mt as abbreviation for mitochondria; Box 1
1293			
1294			
1295 mitochondrial outer membrane	mtOM		MOM is widely used, and M is replaced by mt as abbreviation for mitochondria; Box 1
1296			
1297			
1298 mitochondrial recovery	$Y_{mtE}$		Fig. 9
1299 mitochondrial yield	$Y_{mtE/m}$		Fig. 9
1300 negative	neg		Fig. 2
1301 number concentration of X	$C_{NX}$	[x·m <sup>-3</sup> ]	Tab. 4
1302 number of entities X	$N_X$	[x]	Tab. 4, Fig. 10
1303 number of entity B	$N_B$	[x]	Tab. 4
1304 oxidative phosphorylation	OXPHOS		Tab. 1
1305 oxygen concentration	$c_{O_2} = n_{O_2} \cdot V^{-1}$ ; [O <sub>2</sub> ]	[mol·m <sup>-3</sup> ]	Section 3.2
1306 phosphorylation of ADP to ATP	P»		Section 2.2
1307 positive	pos		Fig. 2
1308 proton in the negative compartment	H <sup>+</sup> <sub>neg</sub>		Fig. 2
1309 proton in the positive compartment	H <sup>+</sup> <sub>pos</sub>		Fig. 2
1310 rate of electron transfer in ET state	$E$		ET-capacity; Tab. 1
1311 rate of LEAK respiration	$L$		Tab. 1
1312 rate of oxidative phosphorylation	$P$		OXPHOS capacity; Tab. 1
1313 rate of residual oxygen consumption	$R_{ox}$		Tab. 1
1314 residual oxygen consumption	ROX		Tab. 1
1315 specific mitochondrial density	$D_{mtE} = mtE \cdot m_X^{-1}$	[mtEU·kg <sup>-1</sup> ]	Tab. 7
1316 volume	$V$	[m <sup>3</sup> ]	
1317 weight, dry weight	$W_d$	[kg]	used as mass of sample X; Fig. 8
1318 weight, wet weight	$W_w$	[kg]	used as mass of sample X; Fig. 8
1319			

1320

1321 Terms and symbols are summarized in **Table 8**. Their use will facilitate transdisciplinary  
 1322 communication and support further developments towards a consistent theory of bioenergetics  
 1323 and mitochondrial physiology. Technical terms related to and defined with normal words can  
 1324 be used as identifiers in databases, support the creation of ontologies towards semantic  
 1325 information processing (MitoPedia), and help in communicating analytical findings as  
 1326 impactful data-driven stories. *‘Making data available without making it understandable may be*  
 1327 *worse than not making it available at all’* (National Academies of Sciences, Engineering, and  
 1328 Medicine 2018). This is a call to carefully contribute to FAIR principles (Findable, Accessible,  
 1329 Interoperable, Reusable) for the sharing of scientific data.

1330

---

### 1331 **Box 3: Mitochondrial and cell respiration**

1332

1333 Mitochondrial and cell respiration is the process of exergonic and exothermic energy  
 1334 transformation in which scalar redox reactions are coupled to vectorial ion translocation across  
 1335 a semipermeable membrane, which separates the small volume of a bacterial cell or  
 1336 mitochondrion from the larger volume of its surroundings. The electrochemical exergy can be  
 1337 partially conserved in the phosphorylation of ADP to ATP or in ion pumping, or dissipated in  
 1338 an electrochemical short-circuit. Respiration is thus clearly distinguished from fermentation as  
 1339 the counterpart of cellular core energy metabolism. Respiration is separated in mitochondrial  
 1340 preparations from the partial contribution of fermentative pathways of the intact cell. Residual  
 1341 oxygen consumption—as measured after inhibition of mitochondrial electron transfer—does  
 1342 not belong to the class of catabolic reactions and is, therefore, subtracted from total oxygen  
 1343 consumption to obtain baseline-corrected respiration.

---

1344

### 1345 **Acknowledgements**

1346 We thank M. Beno for management assistance. Supported by COST Action CA15203  
 1347 MitoEAGLE and K-Regio project MitoFit (E.G.).

1348

1349 **Competing financial interests:** E.G. is founder and CEO of Oroboros Instruments, Innsbruck,  
 1350 Austria.

1351

### 1352 **5. References**

1353

- 1354 Altmann R (1894) Die Elementarorganismen und ihre Beziehungen zu den Zellen. Zweite vermehrte Auflage.  
 1355 Verlag Von Veit & Comp, Leipzig:160 pp.
- 1356 Beard DA (2005) A biophysical model of the mitochondrial respiratory system and oxidative phosphorylation.  
 1357 PLoS Comput Biol 1(4):e36.
- 1358 Benda C (1898) Weitere Mitteilungen über die Mitochondria. Verh Dtsch Physiol Ges:376-83.
- 1359 Birkedal R, Laasmaa M, Vendelin M (2014) The location of energetic compartments affects energetic  
 1360 communication in cardiomyocytes. Front Physiol 5:376.
- 1361 Breton S, Beaupré HD, Stewart DT, Hoeh WR, Blier PU (2007) The unusual system of doubly uniparental  
 1362 inheritance of mtDNA: isn't one enough? Trends Genet 23:465-74.
- 1363 Brown GC (1992) Control of respiration and ATP synthesis in mammalian mitochondria and cells. Biochem J  
 1364 284:1-13.
- 1365 Calvo SE, Klauser CR, Mootha VK (2016) MitoCarta2.0: an updated inventory of mammalian mitochondrial  
 1366 proteins. Nucleic Acids Research 44:D1251-7.
- 1367 Calvo SE, Julien O, Clauser KR, Shen H, Kamer KJ, Wells JA, Mootha VK (2017) Comparative analysis of  
 1368 mitochondrial N-termini from mouse, human, and yeast. Mol Cell Proteomics 16:512-23.
- 1369 Campos JC, Queliconi BB, Bozi LHM, Bechara LRG, Dourado PMM, Andres AM, Jannig PR, Gomes KMS,  
 1370 Zambelli VO, Rocha-Resende C, Guatimosim S, Brum PC, Mochly-Rosen D, Gottlieb RA, Kowaltowski AJ,  
 1371 Ferreira JCB (2017) Exercise reestablishes autophagic flux and mitochondrial quality control in heart failure.  
 1372 Autophagy 13:1304-317.
- 1373 Canton M, Luvisetto S, Schmehl I, Azzone GF (1995) The nature of mitochondrial respiration and  
 1374 discrimination between membrane and pump properties. Biochem J 310:477-81.



- 1375 Chance B, Williams GR (1955a) Respiratory enzymes in oxidative phosphorylation. I. Kinetics of oxygen  
1376 utilization. *J Biol Chem* 217:383-93.
- 1377 Chance B, Williams GR (1955b) Respiratory enzymes in oxidative phosphorylation: III. The steady state. *J Biol*  
1378 *Chem* 217:409-27.
- 1379 Chance B, Williams GR (1955c) Respiratory enzymes in oxidative phosphorylation. IV. The respiratory chain. *J*  
1380 *Biol Chem* 217:429-38.
- 1381 Chance B, Williams GR (1956) The respiratory chain and oxidative phosphorylation. *Adv Enzymol Relat Subj*  
1382 *Biochem* 17:65-134.
- 1383 Cobb LJ, Lee C, Xiao J, Yen K, Wong RG, Nakamura HK, Mehta HH, Gao Q, Ashur C, Huffman DM, Wan J,  
1384 Muzumdar R, Barzilai N, Cohen P (2016) Naturally occurring mitochondrial-derived peptides are age-  
1385 dependent regulators of apoptosis, insulin sensitivity, and inflammatory markers. *Aging (Albany NY)* 8:796-  
1386 809.
- 1387 Cohen ER, Cvitas T, Frey JG, Holmström B, Kuchitsu K, Marquardt R, Mills I, Pavese F, Quack M, Stohner J,  
1388 Strauss HL, Takami M, Thor HL (2008) Quantities, units and symbols in physical chemistry, IUPAC Green  
1389 Book, 3rd Edition, 2nd Printing, IUPAC & RSC Publishing, Cambridge.
- 1390 Cooper H, Hedges LV, Valentine JC, eds (2009) The handbook of research synthesis and meta-analysis. Russell  
1391 Sage Foundation.
- 1392 Coopersmith J (2010) Energy, the subtle concept. The discovery of Feynman's blocks from Leibnitz to Einstein.  
1393 Oxford University Press:400 pp.
- 1394 Cummins J (1998) Mitochondrial DNA in mammalian reproduction. *Rev Reprod* 3:172-82.
- 1395 Dai Q, Shah AA, Garde RV, Yonish BA, Zhang L, Medvitz NA, Miller SE, Hansen EL, Dunn CN, Price TM  
1396 (2013) A truncated progesterone receptor (PR-M) localizes to the mitochondrion and controls cellular  
1397 respiration. *Mol Endocrinol* 27:741-53.
- 1398 Divakaruni AS, Brand MD (2011) The regulation and physiology of mitochondrial proton leak. *Physiology*  
1399 (Bethesda) 26:192-205.
- 1400 Doerrier C, Garcia-Souza LF, Krumschnabel G, Wohlfarter Y, Mészáros AT, Gnaiger E (2018) High-Resolution  
1401 FluoRespirometry and OXPHOS protocols for human cells, permeabilized fibres from small biopsies of  
1402 muscle and isolated mitochondria. *Methods Mol. Biol.* (in press)
- 1403 Doskey CM, van 't Erve TJ, Wagner BA, Buettner GR (2015) Moles of a substance per cell is a highly  
1404 informative dosing metric in cell culture. *PLOS ONE* 10:e0132572.
- 1405 Drahotová Z, Milerová M, Stieglarová A, Houstek J, Ostádal B (2004) Developmental changes of cytochrome *c*  
1406 oxidase and citrate synthase in rat heart homogenate. *Physiol Res* 53:119-22.
- 1407 Duarte FV, Palmeira CM, Rolo AP (2014) The role of microRNAs in mitochondria: small players acting wide.  
1408 *Genes (Basel)* 5:865-86.
- 1409 Ernster L, Schatz G (1981) Mitochondria: a historical review. *J Cell Biol* 91:227s-55s.
- 1410 Estabrook RW (1967) Mitochondrial respiratory control and the polarographic measurement of ADP:O ratios.  
1411 *Methods Enzymol* 10:41-7.
- 1412 Faber C, Zhu ZJ, Castellino S, Wagner DS, Brown RH, Peterson RA, Gates L, Barton J, Bickett M, Hagerty L,  
1413 Kimbrough C, Sola M, Bailey D, Jordan H, Elangbam CS (2014) Cardiolipin profiles as a potential  
1414 biomarker of mitochondrial health in diet-induced obese mice subjected to exercise, diet-restriction and  
1415 ephedrine treatment. *J Appl Toxicol* 34:1122-9.
- 1416 Fell D (1997) Understanding the control of metabolism. Portland Press.
- 1417 Garlid KD, Beavis AD, Ratkje SK (1989) On the nature of ion leaks in energy-transducing membranes. *Biochim*  
1418 *Biophys Acta* 976:109-20.
- 1419 Garlid KD, Semrad C, Zinchenko V. Does redox slip contribute significantly to mitochondrial respiration? In:  
1420 Schuster S, Rigoulet M, Ouhabi R, Mazat J-P, eds (1993) Modern trends in biothermokinetics. Plenum Press,  
1421 New York, London:287-93.
- 1422 Gerö D, Szabo C (2016) Glucocorticoids suppress mitochondrial oxidant production via upregulation of  
1423 uncoupling protein 2 in hyperglycemic endothelial cells. *PLoS One* 11:e0154813.
- 1424 Gnaiger E. Efficiency and power strategies under hypoxia. Is low efficiency at high glycolytic ATP production a  
1425 paradox? In: *Surviving Hypoxia: Mechanisms of Control and Adaptation*. Hochachka PW, Lutz PL, Sick T,  
1426 Rosenthal M, Van den Thillart G, eds (1993a) CRC Press, Boca Raton, Ann Arbor, London, Tokyo:77-109.
- 1427 Gnaiger E (1993b) Nonequilibrium thermodynamics of energy transformations. *Pure Appl Chem* 65:1983-2002.
- 1428 Gnaiger E (2001) Bioenergetics at low oxygen: dependence of respiration and phosphorylation on oxygen and  
1429 adenosine diphosphate supply. *Respir Physiol* 128:277-97.
- 1430 Gnaiger E (2009) Capacity of oxidative phosphorylation in human skeletal muscle. New perspectives of  
1431 mitochondrial physiology. *Int J Biochem Cell Biol* 41:1837-45.
- 1432 Gnaiger E (2014) Mitochondrial pathways and respiratory control. An introduction to OXPHOS analysis. 4th ed.  
1433 *Mitochondr Physiol Network* 19.12. Oroboros MiPNet Publications, Innsbruck:80 pp.
- 1434 Gnaiger E, Méndez G, Hand SC (2000) High phosphorylation efficiency and depression of uncoupled respiration  
1435 in mitochondria under hypoxia. *Proc Natl Acad Sci USA* 97:11080-5.

- 1436 Greggio C, Jha P, Kulkarni SS, Lagarrigue S, Broskey NT, Boutant M, Wang X, Conde Alonso S, Ofori E,  
1437 Auwerx J, Cantó C, Amati F (2017) Enhanced respiratory chain supercomplex formation in response to  
1438 exercise in human skeletal muscle. *Cell Metab* 25:301-11.
- 1439 Hinkle PC (2005) P/O ratios of mitochondrial oxidative phosphorylation. *Biochim Biophys Acta* 1706:1-11.
- 1440 Hofstadter DR (1979) Gödel, Escher, Bach: An eternal golden braid. A metaphorical fugue on minds and  
1441 machines in the spirit of Lewis Carroll. Harvester Press:499 pp.
- 1442 Illaste A, Laasmaa M, Peterson P, Vendelin M (2012) Analysis of molecular movement reveals latticelike  
1443 obstructions to diffusion in heart muscle cells. *Biophys J* 102:739-48.
- 1444 Jasienski M, Bazzaz FA (1999) The fallacy of ratios and the testability of models in biology. *Oikos* 84:321-26.
- 1445 Jepihhina N, Beraud N, Sepp M, Birkedal R, Vendelin M (2011) Permeabilized rat cardiomyocyte response  
1446 demonstrates intracellular origin of diffusion obstacles. *Biophys J* 101:2112-21.
- 1447 Klepinin A, Ounpuu L, Guzun R, Chekulayev V, Timohhina N, Tepp K, Shevchuk I, Schlattner U, Kaambre T  
1448 (2016) Simple oxygraphic analysis for the presence of adenylate kinase 1 and 2 in normal and tumor cells. *J*  
1449 *Bioenerg Biomembr* 48:531-48.
- 1450 Klingenberg M (2017) UCPI - A sophisticated energy valve. *Biochimie* 134:19-27.
- 1451 Koit A, Shevchuk I, Ounpuu L, Klepinin A, Chekulayev V, Timohhina N, Tepp K, Puurand M, Truu L, Heck K,  
1452 Valvere V, Guzun R, Kaambre T (2017) Mitochondrial respiration in human colorectal and breast cancer  
1453 clinical material is regulated differently. *Oxid Med Cell Longev* 1372640.
- 1454 Komlódi T, Tretter L (2017) Methylene blue stimulates substrate-level phosphorylation catalysed by succinyl-  
1455 CoA ligase in the citric acid cycle. *Neuropharmacology* 123:287-98.
- 1456 Lane N (2005) Power, sex, suicide: mitochondria and the meaning of life. Oxford University Press:354 pp.
- 1457 Larsen S, Nielsen J, Neigaard Nielsen C, Nielsen LB, Wibrand F, Stride N, Schroder HD, Boushel RC, Helge  
1458 JW, Dela F, Hey-Mogensen M (2012) Biomarkers of mitochondrial content in skeletal muscle of healthy  
1459 young human subjects. *J Physiol* 590:3349-60.
- 1460 Lee C, Zeng J, Drew BG, Sallam T, Martin-Montalvo A, Wan J, Kim SJ, Mehta H, Hevener AL, de Cabo R,  
1461 Cohen P (2015) The mitochondrial-derived peptide MOTS-c promotes metabolic homeostasis and reduces  
1462 obesity and insulin resistance. *Cell Metab* 21:443-54.
- 1463 Lee SR, Kim HK, Song IS, Youm J, Dizon LA, Jeong SH, Ko TH, Heo HJ, Ko KS, Rhee BD, Kim N, Han J  
1464 (2013) Glucocorticoids and their receptors: insights into specific roles in mitochondria. *Prog Biophys Mol*  
1465 *Biol* 112:44-54.
- 1466 Leek BT, Mudaliar SR, Henry R, Mathieu-Costello O, Richardson RS (2001) Effect of acute exercise on citrate  
1467 synthase activity in untrained and trained human skeletal muscle. *Am J Physiol Regul Integr Comp Physiol*  
1468 280:R441-7.
- 1469 Lemieux H, Blier PU, Gnaiger E (2017) Remodeling pathway control of mitochondrial respiratory capacity by  
1470 temperature in mouse heart: electron flow through the Q-junction in permeabilized fibers. *Sci Rep* 7:2840.
- 1471 Lenaz G, Tioli G, Falasca AI, Genova ML (2017) Respiratory supercomplexes in mitochondria. In: *Mechanisms*  
1472 *of primary energy trasduction in biology*. M Wikstrom (ed) Royal Society of Chemistry Publishing, London,  
1473 UK:296-337.
- 1474 Margulis L (1970) Origin of eukaryotic cells. New Haven: Yale University Press.
- 1475 Meinild Lundby AK, Jacobs RA, Gehrig S, de Leur J, Hauser M, Bonne TC, Flück D, Dandanell S, Kirk N,  
1476 Kaech A, Ziegler U, Larsen S, Lundby C (2018) Exercise training increases skeletal muscle mitochondrial  
1477 volume density by enlargement of existing mitochondria and not de novo biogenesis. *Acta Physiol* 222,  
1478 e12905.
- 1479 Menshikova EV, Ritov VB, Fairfull L, Ferrell RE, Kelley DE, Goodpaster BH (2006) Effects of exercise on  
1480 mitochondrial content and function in aging human skeletal muscle. *J Gerontol A Biol Sci Med Sci* 61:534-  
1481 40.
- 1482 Menshikova EV, Ritov VB, Ferrell RE, Azuma K, Goodpaster BH, Kelley DE (2007) Characteristics of skeletal  
1483 muscle mitochondrial biogenesis induced by moderate-intensity exercise and weight loss in obesity. *J Appl*  
1484 *Physiol* (1985) 103:21-7.
- 1485 Menshikova EV, Ritov VB, Toledo FG, Ferrell RE, Goodpaster BH, Kelley DE (2005) Effects of weight loss  
1486 and physical activity on skeletal muscle mitochondrial function in obesity. *Am J Physiol Endocrinol Metab*  
1487 288:E818-25.
- 1488 Miller GA (1991) The science of words. Scientific American Library New York:276 pp.
- 1489 Mitchell P (1961) Coupling of phosphorylation to electron and hydrogen transfer by a chemi-osmotic type of  
1490 mechanism. *Nature* 191:144-8.
- 1491 Mitchell P (2011) Chemiosmotic coupling in oxidative and photosynthetic phosphorylation. *Biochim Biophys*  
1492 *Acta Bioenergetics* 1807:1507-38.
- 1493 Mogensen M, Sahlin K, Fernström M, Glintborg D, Vind BF, Beck-Nielsen H, Højlund K (2007) Mitochondrial  
1494 respiration is decreased in skeletal muscle of patients with type 2 diabetes. *Diabetes* 56:1592-9.
- 1495 Mohr PJ, Phillips WD (2015) Dimensionless units in the SI. *Metrologia* 52:40-7.
- 1496 Moreno M, Giacco A, Di Munno C, Goglia F (2017) Direct and rapid effects of 3,5-diiodo-L-thyronine (T2).  
1497 *Mol Cell Endocrinol* 7207:30092-8.

- 1498 Morrow RM, Picard M, Derbeneva O, Leipzig J, McManus MJ, Gousspillou G, Barbat-Artigas S, Dos Santos C,  
 1499 Hepple RT, Murdock DG, Wallace DC (2017) Mitochondrial energy deficiency leads to hyperproliferation of  
 1500 skeletal muscle mitochondria and enhanced insulin sensitivity. *Proc Natl Acad Sci U S A* 114:2705-10.
- 1501 Murley A, Nunnari J (2016) The emerging network of mitochondria-organelle contacts. *Mol Cell* 61:648-53.
- 1502 National Academies of Sciences, Engineering, and Medicine (2018) International coordination for science data  
 1503 infrastructure: Proceedings of a workshop—in Brief. Washington, DC: The National Academies Press. doi:  
 1504 <https://doi.org/10.17226/25015>.
- 1505 Paradies G, Paradies V, De Benedictis V, Ruggiero FM, Petrosillo G (2014) Functional role of cardiolipin in  
 1506 mitochondrial bioenergetics. *Biochim Biophys Acta* 1837:408-17.
- 1507 Pesta D, Gnaiger E (2012) High-Resolution Respirometry. OXPHOS protocols for human cells and  
 1508 permeabilized fibres from small biopsies of human muscle. *Methods Mol Biol* 810:25-58.
- 1509 Pesta D, Hoppel F, Macek C, Messner H, Faulhaber M, Kobel C, Parson W, Burtscher M, Schocke M, Gnaiger  
 1510 E (2011) Similar qualitative and quantitative changes of mitochondrial respiration following strength and  
 1511 endurance training in normoxia and hypoxia in sedentary humans. *Am J Physiol Regul Integr Comp Physiol*  
 1512 301:R1078–87.
- 1513 Price TM, Dai Q (2015) The role of a mitochondrial progesterone receptor (PR-M) in progesterone action.  
 1514 *Semin Reprod Med* 33:185-94.
- 1515 Puchowicz MA, Varnes ME, Cohen BH, Friedman NR, Kerr DS, Hoppel CL (2004) Oxidative phosphorylation  
 1516 analysis: assessing the integrated functional activity of human skeletal muscle mitochondria – case studies.  
 1517 *Mitochondrion* 4:377-85. Puntschart A, Claassen H, Jostarndt K, Hoppeler H, Billeter R (1995) mRNAs of  
 1518 enzymes involved in energy metabolism and mtDNA are increased in endurance-trained athletes. *Am J*  
 1519 *Physiol* 269:C619-25.
- 1520 Quiros PM, Mottis A, Auwerx J (2016) Mitonuclear communication in homeostasis and stress. *Nat Rev Mol*  
 1521 *Cell Biol* 17:213-26.
- 1522 Reichmann H, Hoppeler H, Mathieu-Costello O, von Bergen F, Pette D (1985) Biochemical and ultrastructural  
 1523 changes of skeletal muscle mitochondria after chronic electrical stimulation in rabbits. *Pflugers Arch* 404:1-  
 1524 9.
- 1525 Renner K, Amberger A, Konwalinka G, Gnaiger E (2003) Changes of mitochondrial respiration, mitochondrial  
 1526 content and cell size after induction of apoptosis in leukemia cells. *Biochim Biophys Acta* 1642:115-23.
- 1527 Rich P (2003) Chemiosmotic coupling: The cost of living. *Nature* 421:583.
- 1528 Rostovtseva TK, Sheldon KL, Hassanzadeh E, Monge C, Saks V, Bezrukov SM, Sackett DL (2008) Tubulin  
 1529 binding blocks mitochondrial voltage-dependent anion channel and regulates respiration. *Proc Natl Acad Sci*  
 1530 *USA* 105:18746-51.
- 1531 Rustin P, Parfait B, Chretien D, Bourgeron T, Djouadi F, Bastin J, Rötig A, Munnich A (1996) Fluxes of  
 1532 nicotinamide adenine dinucleotides through mitochondrial membranes in human cultured cells. *J Biol Chem*  
 1533 271:14785-90.
- 1534 Saks VA, Veksler VI, Kuznetsov AV, Kay L, Sikk P, Tiivel T, Tranqui L, Olivares J, Winkler K, Wiedemann F,  
 1535 Kunz WS (1998) Permeabilised cell and skinned fiber techniques in studies of mitochondrial function in  
 1536 vivo. *Mol Cell Biochem* 184:81-100.
- 1537 Salabei JK, Gibb AA, Hill BG (2014) Comprehensive measurement of respiratory activity in permeabilized cells  
 1538 using extracellular flux analysis. *Nat Protoc* 9:421-38.
- 1539 Sazanov LA (2015) A giant molecular proton pump: structure and mechanism of respiratory complex I. *Nat Rev*  
 1540 *Mol Cell Biol* 16:375-88.
- 1541 Schneider TD (2006) Claude Shannon: biologist. The founder of information theory used biology to formulate  
 1542 the channel capacity. *IEEE Eng Med Biol Mag* 25:30-3.
- 1543 Schönfeld P, Dymkowska D, Wojtczak L (2009) Acyl-CoA-induced generation of reactive oxygen species in  
 1544 mitochondrial preparations is due to the presence of peroxisomes. *Free Radic Biol Med* 47:503-9.
- 1545 Schultz J, Wiesner RJ (2000) Proliferation of mitochondria in chronically stimulated rabbit skeletal muscle--  
 1546 transcription of mitochondrial genes and copy number of mitochondrial DNA. *J Bioenerg Biomembr* 32:627-  
 1547 34.
- 1548 Simson P, Jepihhina N, Laasmaa M, Peterson P, Birkedal R, Vendelin M (2016) Restricted ADP movement in  
 1549 cardiomyocytes: Cytosolic diffusion obstacles are complemented with a small number of open mitochondrial  
 1550 voltage-dependent anion channels. *J Mol Cell Cardiol* 97:197-203.
- 1551 Stucki JW, Ineichen EA (1974) Energy dissipation by calcium recycling and the efficiency of calcium transport  
 1552 in rat-liver mitochondria. *Eur J Biochem* 48:365-75.
- 1553 Tonkonogi M, Harris B, Sahlin K (1997) Increased activity of citrate synthase in human skeletal muscle after a  
 1554 single bout of prolonged exercise. *Acta Physiol Scand* 161:435-6.
- 1555 Waczulikova I, Habodaszova D, Cagalinec M, Ferko M, Ulicna O, Mateasik A, Sikurova L, Ziegelhöffer A  
 1556 (2007) Mitochondrial membrane fluidity, potential, and calcium transients in the myocardium from acute  
 1557 diabetic rats. *Can J Physiol Pharmacol* 85:372-81.
- 1558 Wagner BA, Venkataraman S, Buettner GR (2011) The rate of oxygen utilization by cells. *Free Radic Biol Med*  
 1559 51:700-712.

- 1560 Wang H, Hiatt WR, Barstow TJ, Brass EP (1999) Relationships between muscle mitochondrial DNA content,  
1561 mitochondrial enzyme activity and oxidative capacity in man: alterations with disease. *Eur J Appl Physiol*  
1562 *Occup Physiol* 80:22-7.
- 1563 Watt IN, Montgomery MG, Runswick MJ, Leslie AG, Walker JE (2010) Bioenergetic cost of making an  
1564 adenosine triphosphate molecule in animal mitochondria. *Proc Natl Acad Sci U S A* 107:16823-7.
- 1565 Weibel ER, Hoppeler H (2005) Exercise-induced maximal metabolic rate scales with muscle aerobic capacity. *J*  
1566 *Exp Biol* 208:1635-44.
- 1567 White DJ, Wolff JN, Pierson M, Gemmell NJ (2008) Revealing the hidden complexities of mtDNA inheritance.  
1568 *Mol Ecol* 17:4925-42.
- 1569 Wikström M, Hummer G (2012) Stoichiometry of proton translocation by respiratory complex I and its  
1570 mechanistic implications. *Proc Natl Acad Sci U S A* 109:4431-6.
- 1571 Willis WT, Jackman MR, Messer JI, Kuzmiak-Glancy S, Glancy B (2016) A simple hydraulic analog model of  
1572 oxidative phosphorylation. *Med Sci Sports Exerc* 48:990-1000.